THE RECOVERY OF MANGANESE FROM LOW GRADE RESOURCES: BENCH SCALE METALLURGICAL TEST PROGRAM COMPLETED

Prepared for:
American Manganese Inc.
2A – 15782 Marine Drive
White Rock, BC
V4B 1E6
CANADA

Prepared by:
Norman Chow, P.Eng.,
Anca Nacu, PhD,
Doug Warkentin, P.Eng.,
Igor Aksenov,
Hoe Teh, P.Eng.
Kemetco Research Inc.
#445 - 5600 Parkwood Way
Richmond, BC
V6V 2M2
CANADA

August 19, 2010

IRAP Project No.: 712681

KEMETCO
RESEARCH INC

August 19, 2010

Mr. Larry W. Reaugh
President & CEO
American Manganese Inc.
2A 15782 Marine Drive
White Rock, BC
V4B 1E6
CANADA

Dear Mr. Reaugh:

Re: Kemetco's Final Report of the Completed Bench Scale Test Program

I am pleased to present this technical report which summarizes Kemetco's bench scale test work on American Manganese Inc's Artillery Peak Project.

The work shows conceptual flowsheets for an integrated novel process to produce high grade electrolytic manganese metal from the Artillery Peak Resource in Arizona. This is a new process containing proprietary intellectual know-how which is the subject of patent protection as we discussed previously. Kemetco made extensive use of existing reports made available from American Manganese Inc., developed and extended the known state of the art through its in-house expertise and resources to achieve what we believe is a totally new conceptual process which provides a sound basis for future work.

As per your request, Kemetco is preparing a proposal to extend this project to include continuous small scale pilot plant demonstration to confirm and extend existing data.

I trust this is satisfactory.

Yours Truly,

Norman Chow, M.A.Sc., P.Eng
President

EXECUTIVE SUMMARY

American Manganese Inc has developed a low-cost, environmentally friendly hydrometallurgical process to recover manganese (Mn) from lower grade resources containing pyrolusite (MnO_2), psilomelane and other four valent Mn oxides. This report describes the results of a metallurgical test program contracted by American Manganese to Kemetco Research Inc. The test program was partially funded by the Canadian Government through the National Research Council, Industrial Research Assistance Program (NRC-IRAP) for development work conducted over a one year period.

The purpose of this program has been to conduct bench scale testing of unit operations, that when combined, form the basis of an innovative conceptual process flow sheet to process lower grade Mn resources into high purity Mn metal in an economically viable manner. The process is designed to treat 3500 metric tonnes per day of resource and will produce 141 metric tonnes per day of Mn metal product, and 366 metric tonnes per day of anhydrous sodium sulphate (Na_2SO_4) crystal by-product.

Treatment of the lower grade American Manganese resource which contains, on average 4% to 7% Mn by weight is carried out in a hydrometallurgical process, where four valent Mn is readily leachable by SO_2 dissolved in water. The hydrometallurgical processing of lower grade material avoids high temperature reduction roasting that is conventionally used in processing high grade material to render the manganese to be acid leachable using sulphuric acid (H_2SO_4). High temperature roasting is energy intensive and would not be economical for lower grade material.

The conceptual process flow sheet developed during this test program is based on a unique application of commercially available process equipment. As such, the process is deemed to be robust, energy efficient, uses minimal water and in addition to production of electrolytic manganese metal will also produce a saleable anhydrous sodium sulphate by-product. The energy to recover water and destroy dithionates is approximately balanced with the energy produced by burning of sulphur (S) to produce SO_2. High energy requirements for these applications were a major challenge facing prior art. Dithionate destruction yields SO_2 which can be recycled to the leaching stage and use of water is minimized thru production of solid tailings which can be returned to worked out areas of the open pit.

Key aspects of the process flowsheet are as follows:

Sulphur Burning

- SO_2 leachant is produced on-site by burning elemental sulphur with 20% excess air.
- Heat exchanging the exhaust gases from the sulphur burner will produce 20 tonnes per hour of steam at 400 °C and 45 bar pressure.
- In a condensing turbine, this steam can produce 5 MW of continuous electrical power.

Leaching

- The Mn mineral in the resource sample provided by American Manganese is primarily pyrolusite and wad (MnO_2), in which the Mn has a 4^+ valence. The insoluble 4^+ valence species of Mn can be readily reduced to soluble 2^+ with an SO_2 reducing agent dissolved in water.
- Leaching studies performed on American Manganese resources of large particle size (greater than 9.5 mm) with dilute SO_2 in stirred tanks indicates that the material is readily leachable, with Mn extractions greater than 90% achieved.
- The material is friable and large particles break down easily during stirred tank leaching. As such crushing and grinding to a fine particle size prior to leaching is not necessary.
- After leaching, the Mn in solution can be separated from the leach residue using a counter current decantation (CCD) circuit that is typically used in mineral processing operations.

Leachant Purification

- Solution purification is performed in two stages. In the first stage, the solution pH is adjusted to above 6 to precipitate aluminum (Al), arsenic (As) and most of the iron (Fe) and silica (SiO_2). Air/oxygen sparging during the pH adjustment will improve the Fe removal, by oxidizing the ferrous iron to its ferric form. In the second stage, sulphide precipitation will remove the zinc (Zn), providing a solution of sufficient purity to process into a saleable product.
- The resource material can be used in the purification stage, by providing sufficient alkalinity to achieve a pH around 6 and precipitate a substantial amount of impurities from solution.

Mn Production

- Mn is separated from the pregnant leach solution (PLS) by precipitation quantitatively as manganese carbonate ($MnCO_3$). This is achieved by mixing sodium carbonate (Na_2CO_3) with the PLS solution.
- Na_2SO_4 and sodium dithionate ($Na_2S_2O_6$) solution by-product is produced during the precipitation of $MnCO_3$.
- Dissolving the $MnCO_3$ with recycled electrolyte produces a Mn containing solution that is conducive to producing high grade Mn metal.
- A scoping electrowinning test using the American Manganese purified leachate yielded a Mn metal product of greater than 99% purity.
- Using typical commercial electrowinning conditions, a sheet of manganese metal was plated over a 24 hour period at a current efficiency of up to 67%. This represents typical commercial performance.
- The Mn metal was plated without the addition of toxic selenium (Se), which is known to improve current efficiency.

Water Recovery & Dithionate Destruction

- Most of the water used in the process becomes Na_2SO_4 and $Na_2S_2O_6$ solution which is produced during the recovery of $MnCO_3$ by precipitation.
- Water recovery from this solution can be achieved with high energy efficiency because of the unique solubility characteristics of Na_2SO_4, enabling the majority of Na_2SO_4 to be crystallized as sodium sulphate decahydrate ($Na_2SO_4\cdot10H_2O$) by cooling the solution. This method is significantly more energy efficient than standard evaporation since it avoids latent heat requirements which accounts for about 85% of the energy required to evaporate water from a starting temperature of 25 ^oC.
- $Na_2S_2O_6$ will report with the $Na_2SO_4\cdot10H_2O$ crystals and can be calcined with high energy efficiency since the majority of water has been removed. Calcining $Na_2S_2O_6$ will produce anhydrous Na_2SO_4 and recover SO_2 which can be recycled back to the leach.

Tailings

- Solid tailings with minimum water content are produced by filtration of the final CCD underflow material, minimizing water requirements for the overall process.
- The solid tailings produced from test work were shown to be benign by the Toxicity Characteristic Leaching Procedure (TCLP).

Future Developments

- Proof of concept was achieved by using a bioreactor technology owned by Kemetco to recover H_2S from $Na_2S_2O_6$. The H_2S can be burned to generate energy and recover SO_2 for leaching. Further development work is required to determine if the reaction rates are adequate for integration into the overall process. Implementation of this technology would further improve the efficiency of the overall process.
- Minor adjustments to the flowsheet developed will enable the production of other products such as ferromanganese or electrolytic manganese dioxide if desired.

Based on the successful test work, conceptual flowsheets have been developed which include applications of novel, proprietary, innovative technology to minimize process operating costs through low water use, low overall energy use and economic destruction of unwanted by-products. Heat produced from burning of sulphur to make SO_2 is essentially in balance with energy required within the process, excluding the energy required for electrowinning. Waste products are minimized enabling cash costs of production of Mn metal to be significantly lower than costs needed to produce high grade Mn metal from traditional processes. Accordingly, American Manganese Inc. has requested Kemetco to file application for patent protection. American Manganese is grateful for the financial support given by the Canadian Government’s National Research Council under its IRAP program.

TABLE OF CONTENTS

LIST OF TABLES

LIST OF FIGURES

1 INTRODUCTION

American Manganese Inc is developing a low-cost, environmentally friendly hydrometallurgical process to recover manganese from lower grade resources containing pyrolusite (MnO_2) and other manganese oxides. As part of the development work, American Manganese contracted Kemetco Research Inc. to undertake an extensive metallurgical test program. The purpose of this program has been to conduct bench scale testing of unit operations, that when combined, form the basis of a complete conceptual process flow sheet to process lower grade Mn resources into high purity Mn metal in a robust and economically viable manner.

Based on the successful test work, conceptual flowsheets have been developed which include applications of treatment strategies to minimize capital and operating costs:

- through the use of commercially available robust equipment
- minimizing corrosive environments in major capital items of equipment
- low water use
- low overall energy use
- economic destruction of unwanted by-products.

The lower capital and operating costs estimated from these flowsheets provides a significant opportunity for American Manganese to advance commercialization efforts to capitalize on its Artillery Peak manganese properties in Arizona. Other manganese resources containing pyrolusite, psilomelane and wad mineralization may present additional opportunities.

This document provides a detailed description of the flowsheets developed as a result of this program, as well as supporting experimental data and calculations. These flowsheets incorporate a unique assembly of modern available commercial technologies, and as such, will be the subject of patent applications for economical recovery of Mn from lower grade resources.

1.1 BACKGROUND

Approximately 90% of global production of manganese is used in the production of iron and steel as a deoxidizer, desulfidizer and alloying agent. Approximately 10 kg of Mn is used per metric tonne of steel produced[1] . As such, it is estimated that about 13 million metric tonnes of manganese is consumed worldwide annually for steel production alone. This makes manganese the fourth most used metal.

The majority of manganese production comes from South Africa, Australia, Gabon and China, where the resource is mostly mined as high grade ore (> 35% Mn by weight). The conventional process for recovering electrolytic Mn from these sources involves high temperature reduction roasting[2] of the residual fines (after lump material is screened and shipped for ferromanganese production) to render naturally occurring higher valent manganese species (Mn^{3+} to Mn^{4+}) to be reduced to Mn^{2+} which is leachable by sulphuric acid. This roasting operation at temperatures 800 – 1000 °C is very energy intensive, and as such, is only economically feasible for processing of high grade resources, generally Mn > 35% by weight. The Artillery Peak manganese resource is almost entirely composed of pyrolusite, psilomelane and wad which is four-valent manganese easily reduced to two-valent Mn by aqueous sulphur dioxide solution at ambient temperature. Dissolution is fast and almost complete from particles which have been crushed to approximately 30 mm but not milled through conventional ball or rod mill circuit.

The recovery of manganese from lower grade resources has been studied for a number of years. Henn et al[3] provides a detailed review of major proposed processes for recovering manganese from lower grade resources using hydrometallurgical techniques. The report by Henn et al makes reference to forty eight research reports, with a significant number by the U.S. Bureau of Mines. Pahlman[4] et al, in a more recent U.S. Bureau of Mines report, provides detailed reactions that take place when leaching Mn^{4+} minerals with SO_2 dissolved in water. The motivation for the prior work was to develop a process to provide North American steelmakers with a stable supply of manganese from lower grade domestic resources in the event of imported supplies becoming unavailable. North American steelmakers are solely dependent on foreign sources of manganese to meet their requirements for making steel. There is no substitute for manganese in the steelmaking process.

Of key importance of the prior work in the development of manganese extractive metallurgy, was the discovery that four valent manganese is readily leachable with sulphurous acid, which is a reducing acid formed by dissolving sulphur dioxide (SO_2) in water. Leaching the Mn resource with sulphurous acid eliminates the need for roasting,

---

[1] Roskill Information Services, “Economics of Manganese”, Eleventh Edition, 2008, pp 1-2.

[2] Kirk-Othmer Encyclopedia of Chemical Technology, 5th Edition, John Wiley & Sons Inc., Volume 15, pp 538 - 565

[3] John J. Henn, Ralph C. Kirby, Lindsay D. Norman Jr., “Review of Major Proposed Processes for Recovering Manganese from United States Resources”, U.S. Bureau of Mines, Information Circular 8368, 1968

[4] John E. Pahlman, Sanaa E. Khalafalla, “Leaching of Domestic Manganese Ores with Dissolved SO2”, U.S. Bureau of Mines, RI 9150, 1988

and as such vastly improves the potential for economic recovery of Mn from lower grade resources.

The important reactions occurring when Artillery Peak manganese resources are leached with aqueous SO_2 are shown in the following two equations:

$$MnO_2 + SO_2 \rightarrow MnSO_4 \qquad (1)$$

$$MnO_2 + 2SO_2 \rightarrow MnS_2O_6 \qquad (2)$$

Reaction 1 is most desirable as Mn is leached into solution with minimum use of SO_2, and because manganese sulphate ($MnSO_4$) in solution can be directly used for electrowinning at the correct concentration. Reaction 2 is less desirable because of the higher consumption of SO_2. The manganese dithionate (MnS_2O_6) precludes proper control for electrowinning high purity Mn metal and must be removed before electrolysis.

Back[5] et al describes methodology to increase or decrease the formation of MnS_2O_6 by altering the leach variables such as resource and SO_2 feed rate, agitation, temperature, pH and use of certain surfactants. As part of this work, bench scale studies were also conducted on minimizing MnS_2O_6 formation by altering process variables. However, it is extremely difficult to completely eliminate MnS_2O_6 formation by reductive leaching of MnO_2 with SO_2 without negatively affecting Mn concentration in solution, acid and alkali consumption, or water usage. Some MnS_2O_6 production should be expected when recovering Mn from MnO_2 by reductive leaching with SO_2. It is important to develop methodology to deal with MnS_2O_6 in a practical manner that can be integrated into an overall, complete hydrometallurgical process which deals with all by-products, including water and waste in an economical manner.

The U.S. Bureau of Mines report by Henn[3] describes different methods of converting MnS_2O_6 to $MnSO_4$. One method describes autoclaving the MnS_2O_6 containing pregnant leach solution at 230 ^{o}C and 600 psi with air. MnS_2O_6 conversion to $MnSO_4$ would proceed according to the following reaction:

$$MnS_2O_6 + \tfrac{1}{2}O_2 + H_2O \rightarrow MnSO_4 + H_2SO_4 \qquad (3)$$

Autoclaving was found to be an effective method of converting MnS_2O_6 to $MnSO_4$ and H_2SO_4. However, challenges in using this method in the process scheme include the design and operating standards required for safe use of a pressure vessel, and the use of expensive materials to prevent corrosion. These factors can be overcome as autoclaves are widely used in other processes. Process challenges with this technique include inefficient use of SO_2 and potential precipitation of Mn due to its inverse solubility with increasing temperature (see Figure 1)[6]. Controlling optimum concentration of Mn in solution is desirable for electrowinning as is the need to develop an effective scheme to

---

[5] A. E. Back, S.F. Ravitz, K.E. Tame, "Formation of Dithionate and Sulfate in the Oxide of SO2 by MnO2 and Air", U.S. Bureau of Mines, RI 4931, 1952

[6] Grady Tarbutton, J.C. Driskell, T.M. Jones, F.J Gray, C.M. Smith, "Recovery of Sulfur Dioxide from Flue Gases", Industrial and Engineering Chemistry, Vol. 49, No. 3, 1957, pp 395

process the H_2SO_4 by-product in combination with the $MnSO_4$. Henn's report mentions that the H_2SO_4 could be used to consume non-manganese oxides to form insoluble sulphates. This would involve reacting the pregnant leach solution with more resource material in the autoclave. While not mentioned in the Henn report, a perfect balance between H_2SO_4 by-product generation and consumption of non-manganese material to form insoluble products is unlikely. Insufficient acid consuming material would have to be supplemented with the addition of lime to consume excess H_2SO_4. Controlled lime addition would be required as over addition may cause Mn precipitation, resulting in loss of product.

Figure 1:
Solubility of Manganese Sulphate in Water as a Function of Temperature[6].

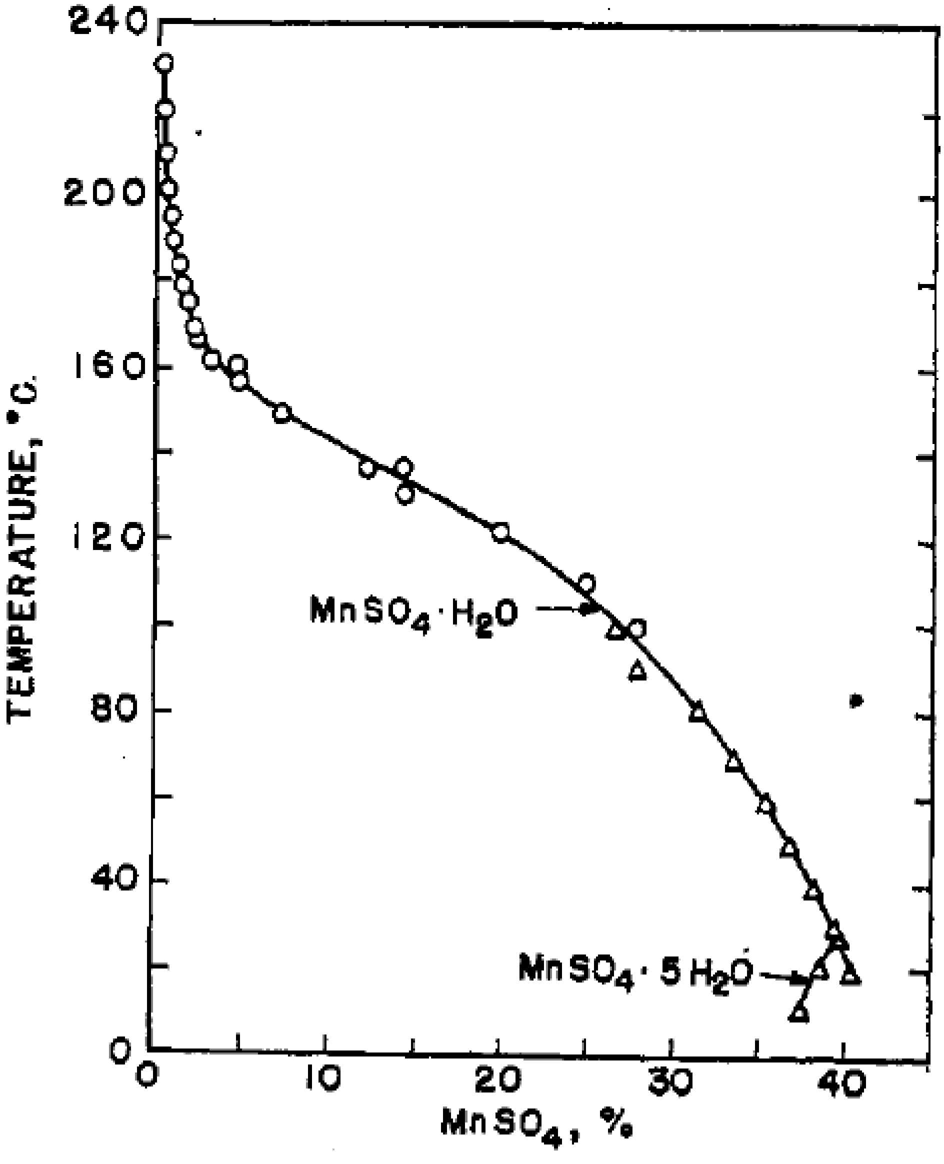

Separation of the H_2SO_4 from the $MnSO_4$ by solvent extraction to make a final by-product of ammonium sulphate ($(NH_4)_2SO_4$) similar to the technique described by Voogt et al for recovering H_2SO_4 from spent nickel electrolyte[7] could be a consideration. The use of Generator Acid Purification technology provided by Eco-Tec[8] to separate H_2SO_4 from Na_2SO_4 could also be considered for use in the process, but is untested for separating H_2SO_4 from $MnSO_4$. In pursuit of a simple robust process scheme, less emphasis and focus has been placed on the use of an autoclave in favor of other potential techniques that could be more easily integrated into a complete process.

A report by Allen[9] describes methodology to evaporate the pregnant leach solution to form $MnSO_4$ and MnS_2O_6 crystals. Sintering the crystals at 1100 to 1200 °C will produce a Mn_3O_4 product as well as evolve SO_2 gas which can be recycled to the leach. The high temperature for sintering was used in this case in order to decompose $MnSO_4$ into Mn_3O_4 and SO_2. As an alternative approach, it would be possible to decompose MnS_2O_6 to form $MnSO_4$ and SO_2 at a much lower temperature[10]. Decomposition starts to occur at temperatures between 140 and 200 °C according to the following reaction:

$$MnS_2O_6 \rightarrow MnSO_4 + SO_2 \qquad (4)$$

This approach would have some benefits for the American Manganese processing scheme as decomposition of MnS_2O_6 can occur at lower temperature. $MnSO_4$ is a desirable intermediate product that can be fed into electrowinning and SO_2 evolution can be recycled back to the leach. The main challenge with this approach is the requirement to evaporate potentially large volumes of water from the pregnant leach solution in order to produce MnS_2O_6 crystal for thermal decomposition. The energy requirement to crystallize MnS_2O_6 by simple evaporation can be significant. In addition, evolution of some SO_2 during evaporation would create a corrosive environment within the evaporator system. Due the large mass handling requirement, the evaporator would likely be an expensive equipment cost for this process. It would be necessary to avoid a corrosive environment in this application.

An additional challenge with this approach would be determining practical methodology to handle the sulphur balance. Dissolving the $MnSO_4$ crystals into solution followed by electrowinning would produce Mn metal and a dilute solution of $MnSO_4$ and H_2SO_4. As discussed earlier in this section, it could be a challenge to perfectly balance consumption of H_2SO_4 to form insoluble sulphates by reacting the dilute $MnSO_4$ and H_2SO_4 solution with the resource material. Additionally, the use of solvent extraction to separate H_2SO_4 from $MnSO_4$ and produce $(NH_4)_2SO_4$ or Generator Acid Purification has not been developed beyond initial bench scale testing in work reported by Hazen Research Inc. (1982-83) for Mn recovery processes.

---

[7] Karen Voogt, Kathryn C. Sole, and Lesley J. Bryson, “Pilot-Plant Study of Sulfuric Acid Extraction from a Nickel Electrolyte Using Alamine 308”, The South African Institute of Mining and Metallurgy, Base Metals Conference, 2009

[8] M. Paleologou, R. Thompson, R.M. Berry, C. Brown, M. Sheedy and T. Gilliss, “The Generator Acid Purification (GAP) System Reduces Caustic Make-up Requirements at Kraft Mills”, Pulp and Paper Canada, Vol. 100:2, 1999, pp 34 - 39

[9] Louis N. Allen, Jr., “Recovery of Manganese from Low-Grade Ores”, Chemical Engineering Progress, Vol 50, No. 1, 1954, pp 9 - 13

[10] R. Gonzales-Santos, R. Roque-Malherbe, “Dielectric Differential Thermal Analysis; VIII. Dithionates”, Journal of Thermal Analysis, Vol. 37, 1991, pp 787-790.

While the prior work provides important information and tested treatment strategies to recover Mn from lower grade resources, the authors of this report have no knowledge or information of any complete process to extract manganese (from lower grade resources in North America) by leaching with aqueous SO_2 and dealing effectively and efficiently with the dithionate content in the course of producing high grade electrolytic manganese metal. Effecting complete control of water and sulphur balances throughout the entire process are important factors to be dealt with in this complete process.

In the development of this robust and cost effective process, the following issues were identified as being key:

- Minimizing the requirements for crushing and grinding
- Leaching the resource with dilute SO_2 formed by combusting sulphur with air
- Defining a simple solid – liquid separation strategy
- Economic destruction of dithionates and recovery of SO_2
- Developing a practical approach for the sulphur balance
- Minimizing water use of the overall process
- Improving the robustness of the process using modern commercial equipment
- Integrating all unit operations into a complete flowsheet

To develop a more robust and cost effective process to recover manganese from lower grade resources, American Manganese contracted Kemetco Research Inc. to undertake an extensive bench scale metallurgical test program to address foregoing issues. The test program was partially funded by the Canadian Government through the National Research Council, Industrial Research Assistance Program (NRC-IRAP) for development work successfully completed over a one year period.

This document provides a detailed description of the flowsheets developed as a result of this program, as well as supporting experimental data and calculations. The process flowsheets describe a significantly improved treatment strategy over prior art, in terms of a more operable, robust process and lower costs. These flowsheets incorporate a unique assembly of modern commercial technologies, and as such, are the subject of patent applications for economical recovery of Mn from abundant lower grade resources known to exist in North America.

2 PROCESS FLOWSHEETS

2.1 AMERICAN MANGANESE PROCESS FLOWSHEET

Figure 2 illustrates the main process flowsheet developed for American Manganese for the recovery of Mn from lower grade resources. A description of the flowsheet is summarized as follows:

Milling Circuit

The resource material provided by American Manganese was sourced from the Artillery Peak deposit in Arizona. This material was found to be clayey and easily broken into fine particles. As such, a simple milling circuit concept is employed, that consists of trucking the run of mine (ROM) material from the open pit and feeding through a grizzly into a feeder bin. Oversized material is crushed by forcing the material through the grizzly grates with a bulldozer. The material is then fed through a hammermill and trommel screen. Minus 30 mm material is stockpiled for feed into the leach system, whereas oversized material is recycled back to the hammermill.

Sulphuric Acid Pre-Leach

The minus 30 mm material is pre-leached with H_2SO_4 solution in stirred tanks. The pulp density will be somewhere between 12 to 20% by weight to facilitate subsequent solid liquid separation with a leach thickener. The material breaks down to finer particle size as a result of the agitation in this stage. Acid consuming material (mainly calcium) reacts with the H_2SO_4 to form insoluble sulphates. The make-up water for the pre-leach comes from the counter current decantation (CCD) wash and will contain manganese recovered from washing the gangue material.

Reductive Leach with SO_2

The pre-leached slurry will cascade to the reductive leach circuit, which consists of a series of stirred tanks. SO_2 gas is sparged into the slurry of the first leach tank to leach the MnO_2 minerals according to Reactions 1 and 2 shown earlier. Unused SO_2 will be collected from the head space of each leach tank and recycled into each subsequent leach tank. The SO_2 depleted gas is then sent do a scrubber after the final leach tank. The SO_2 reducing agent used in the process is produced by combusting elemental sulphur with 20% excess air. This will produce a mixture of 17.5% SO_2, 79.0% N_2 and 3.5% O_2 by volume. Heat exchanging the exhaust gas will produce 20 tonnes per hour of steam at 400 ^oC and 45 bar pressure. In a condensing turbine, this steam can produce 5 MW of continuous electrical power. An additional 2.2 MW of low grade heat is also available for thermal applications below 400 ^oC. This heat recovery is established practice in SO_2 and H_2SO_4 production from burning sulphur.

Leach Thickener

After the leaching stage, the slurry enters a thickener to substantially separate the pregnant leach solution (PLS) from the leached solids. Adequate settling is achieved by operating at a lower pulp density (in the range of 12 to 20% by weight) without the need for auto-dilution (by recycling of the overflow back to the same thickener) to increase settling rates. Although the pulp density is low, the Mn concentration is maintained at an adequately high level in the PLS. Incoming water used in the leach contains Mn recovered from the CCD wash.

Counter Current Decantation

The underflow from the leach thickener containing leached solids and entrained PLS is washed through a multistage (4 to 5 stage) CCD circuit. Clean recycled wash water is used to rinse the solids to recover entrained PLS, while providing an adequately low pulp density to facilitate settling without auto-dilution. The target pulp density is in the range of 12 to 20% by weight. The wash solution containing recovered Mn is recycled back to the leach stage. The solid tailings with minimum water content are produced by filtration of the final CCD underflow, minimizing water requirements of the overall process. The tailings can then be mixed with waste aggregate and cement to create a high density paste fill which is returned to the worked out areas of the open pit. Tailings are benign with no ability to generate acid through oxidation.

Pregnant Leach Solution Purification

The removal of impurities from the PLS is accomplished in two stages. In the first stage, Al, As and SiO_2 are precipitated by raising the pH to 6 in a mix tank. Aeration promotes the precipitation of iron. Soluble ferrous iron is oxidized to less soluble ferric iron. The increase in pH can be achieved by adding the resource material, which has sufficient alkalinity to raise the pH, or by addition of lime. The solid precipitates are separated from the treated PLS in a thickener. The overflow solution is then reacted in a mix tank with NaHS to precipitate Zn as ZnS. The sulphide precipitates are also separated with a thickener and the treated PLS is filtered with a polishing sand filter to remove fine precipitate, resulting a purified PLS containing mainly $MnSO_4$ and MnS_2O_6 solution.

Carbonate Precipitation

Manganese is separated from the PLS by precipitation of solid $MnCO_3$. This is achieved by mixing sodium carbonate with the PLS. Precipitation proceeds according to the following reactions:

$$MnSO_4 + Na_2CO_3 \rightarrow MnCO_3 + Na_2SO_4 \qquad (5)$$

$$MnS_2O_6 + Na_2CO_3 \rightarrow MnCO_3 + Na_2S_2O_6 \qquad (6)$$

In precipitating the $MnCO_3$ a solution by-product containing Na_2SO_4 and $Na_2S_2O_6$ is produced. The solid $MnCO_3$ is separated from the Na_2SO_4 and $Na_2S_2O_6$ by-product solution with a thickener. The wet $MnCO_3$ containing underflow is then dewatered in a filtration system and rinsed producing a clean $MnCO_3$ intermediate product for feed into the electrowinning circuit.

Electrowinning Circuit

The electrowinning circuit for producing Mn metal in the American Manganese process has been designed to operate as an independent, closed loop circuit. This is achieved by maintaining an inventory of $MnCO_3$ feed material that is generated beforehand in the overall process. Operating in this manner significantly improves overall process robustness as the electrowinning circuit can continue to operate should there be process upsets elsewhere. In addition, precise solution concentrations, which are critical to successful electrowinning of Mn metal can be achieved with simple process control. The properties of the $MnCO_3$ material will be very consistent, even with process upsets in the leaching circuit.

In the American Manganese electrowinning scheme, $MnCO_3$ is dissolved with spent electrolyte that is recycled from the electrowinning cells. The $MnCO_3$ feed, recycled electrolyte and required additives will be in balance except for evaporative losses and drag-out. A small amount of make-up material, if required can be easily added during the make-up of fresh $MnSO_4$ electrolyte for the electrowinning process. The electrolyte will contain $(NH_4)_2SO_4$ as a pH buffer and sulphite as a reducing agent to prevent oxidation of Mn in the bulk solution.

The electrolyte is further purified in two stages to remove impurities that may have concentrated into the $MnCO_3$ material during precipitation. Al, As and Fe are removed by adjusting the pH to about 6 and sparging air. The solid precipitates are separated from the solution with a thickener. The solution is then purified a second time with the addition of NaHS to remove Zn as ZnS. After separation of the solids with another thickener, the solution will be of sufficient purity for the electrowinning of high grade Mn metal.

The purified solution will be introduced into the cathode compartment of the divided electrowinning cell. The spent catholyte with lower Mn concentration will be fed into the anolyte to complete the electrochemical cell and regenerate H_2SO_4 which will be recycled back to dissolve $MnCO_3$ for electrolyte make-up.

The main electrochemical reactions are as follows:

Main Cathode Reaction

$$Mn^{2+} + 2e^- \rightarrow Mn \qquad (7)$$

Anode Reaction

$$H_2O \rightarrow \tfrac{1}{2} O_2 + 2H^+ + 2e^- \qquad (8)$$

Net Reaction:

$$MnSO_4 + H_2O \rightarrow Mn + H_2SO_4 + \tfrac{1}{2} O_2 \qquad (9)$$

As the electrowinning of Mn metal only proceeds at about 60 to 70% current efficiency, the following side cathodic reaction will occur:

Side Cathodic Reaction

$$2H_2O + 2e^- \rightarrow H_2 + 2OH^- \qquad (10)$$

The hydroxide (OH^-) generated by the side cathodic reaction introduces a risk for loss of pH control in the cathode compartment. Loss of pH control would cause Mn precipitation on the cathode surface as manganese hydroxide ($Mn(OH)_2$). This would foul the electrode surface and prevent proper electrowinning of Mn metal. To minimize the risk for loss of pH control, the $(NH_4)_2SO_4$ will buffer some of the OH^- generation. In addition, operating within an acceptable range of Mn^{2+} concentration in the cathode compartment is important. If the concentration is too high, Mn precipitation may occur. If the concentration is too low, the generation of OH^- is promoted, which will also promote Mn precipitation. The typical operating conditions for electrowinning Mn metal are provided in Table 1[2].

Table 1:
Typical Conditions for Electrowinning Mn Metal[2]

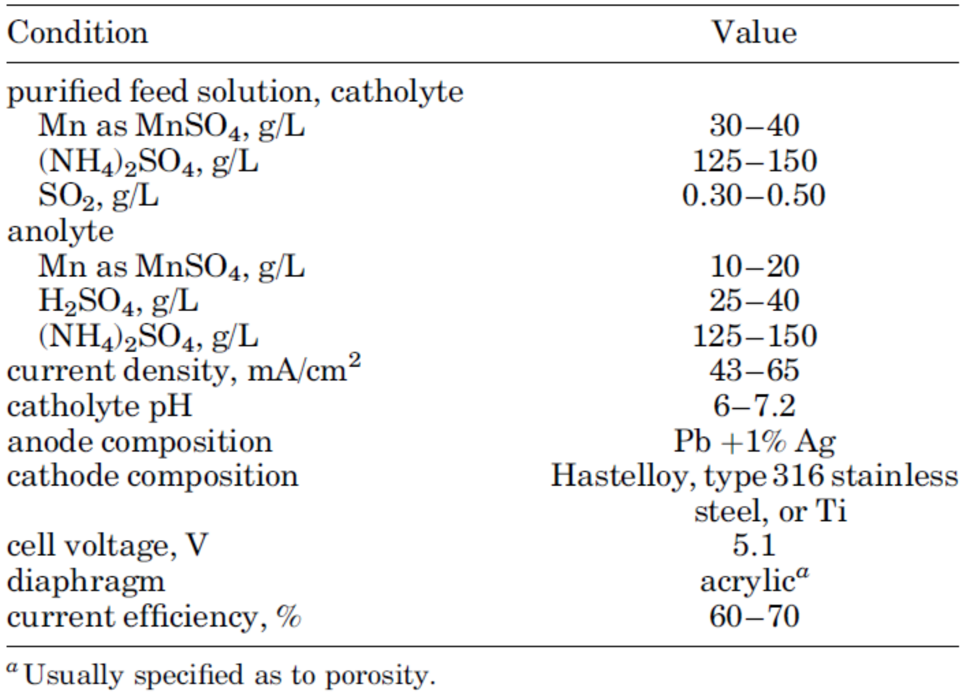

Condition	Value
purified feed solution, catholyte	
Mn as $MnSO_4$, g/L	30–40
$(NH_4)_2SO_4$, g/L	125–150
SO_2, g/L	0.30–0.50
anolyte	
Mn as $MnSO_4$, g/L	10–20
H_2SO_4, g/L	25–40
$(NH_4)_2SO_4$, g/L	125–150
current density, mA/cm^2	43–65
catholyte pH	6–7.2
anode composition	Pb +1% Ag
cathode composition	Hastelloy, type 316 stainless steel, or Ti
cell voltage, V	5.1
diaphragm	acrylic[a]
current efficiency, %	60–70

[a] Usually specified as to porosity.

Water Recovery, Anhydrous Na_2SO_4 Production and Destruction of $Na_2S_2O_6$

The American Manganese process recovers water and destroys dithionates at significantly higher energy efficiency than other processes described in prior art. Efficient water recovery and destruction of dithionates with SO_2 recycle is one of the key aspects that enable the American Manganese process to achieve a low cost of production of Mn from lower grade resources.

Most of the water used in the overall process occurs in the Na_2SO_4 and $Na_2S_2O_6$ containing solution that is produced after precipitation of $MnCO_3$. Water recovery is achieved at high energy efficiency by significantly avoiding the high latent heat requirements required by evaporation of water. Na_2SO_4 has a unique solubility curve that exhibits a significant decrease in solubility with decreasing temperature. As such, most of Na_2SO_4 along with a significant amount of $Na_2S_2O_6$ can be crystallized as a solid by cooling the solution.

The remaining mother solution containing the remaining dissolved Na_2SO_4 and $Na_2S_2O_6$ will be of low salinity. As such, complete recovery of the remaining Na_2SO_4 and $Na_2S_2O_6$ along with clean recycled water can be achieved efficiently by running the mother solution through a nanofiltration system. The Na_2SO_4 and $Na_2S_2O_6$ concentrate can be recycled to the chiller for crystallization, whereas the permeate will consist of clean water which can be used to rinse the tailings and be reused in the leaching process.

The crystal products from the chiller will contain sodium sulphate decahydrate ($Na_2SO_4 \cdot 10H_2O$) and sodium dithionate dihydrate ($Na_2S_2O_6 \cdot 2H_2O$). The $Na_2SO_4 \cdot 10H_2O$ dehydrates at 32.38 ^oC, as such heating the crystals to about 40 ^oC will enable a significant amount of water to be recovered from the crystals. The remaining solids will consist of Anhydrous Na2SO4 and $Na_2S_2O_6 \cdot 2H_2O$, which will be calcined at 267 ^oC to convert the remaining $Na_2S_2O_6 \cdot 2H_2O$ to Anhydrous Na_2SO_4, SO_2 and a small amount of H_2O. The SO_2 and H_2O will be recycled to the leach.

To illustrate the significant energy savings, an initial energy balance comparing water recovery by simple evaporation versus American Manganese's recovery process is summarized in Table 2. In the American Manganese Process, the power required to recover water and destroy dithionates (4.54 MW) is roughly balanced with the electrical power generated from the sulphur burner (5 MW).

Table 2:
Comparison of Power Requirements by Simple Evaporation versus American Manganese's Water Recovery and Dithionate Destruction Process.
Basis for Calculation: 140 Metric Tonnes per Day of Mn Production and 50 g/L Mn for the Pregnant Leachate.

Power Requirement for Simple Evaporation	**MW**
Specific Heat to Raise Temperature From 25 °C to 100 °C	8.83
Latent Heat Requirements for Simple Evaporation	63.53
Low Grade Heat Recovery from Sulphur Burner Exhaust to 100 °C	-1.79
Total Power with Simple Evaporation	**70.57**
American Manganese Water Recovery and Dithionate Destruction Process	**MW**
Power to Chill Na_2SO_4 + $Na_2S_2O_6$ Solution from 25 °C to 0 °C and Crystallize $Na_2SO_4 \cdot 10H_2O$ and $Na_2S_2O_6 \cdot 2H_2O$	7.77
Power to Heat Crystals from 0 °C to 40 °C	0.60
Power for Nanofiltration	0.25
Power to Calcine Na_2SO_4 and $Na_2S_2O_6 \cdot 2H_2O$ Crystals to 267 °C	1.55
Heat Recovery from Mother Liquid at 0 °C	-4.34
Low Grade Heat Recovery from Sulphur Burner Exhaust for Calcine	-0.81
Low Grade Heat Recovery from Sulphur Burner Exhaust for Heating Crystals	-0.60
Total Power with American Manganese Process	**4.42**

Figure 2:
American Manganese Main Conceptual Flowsheet

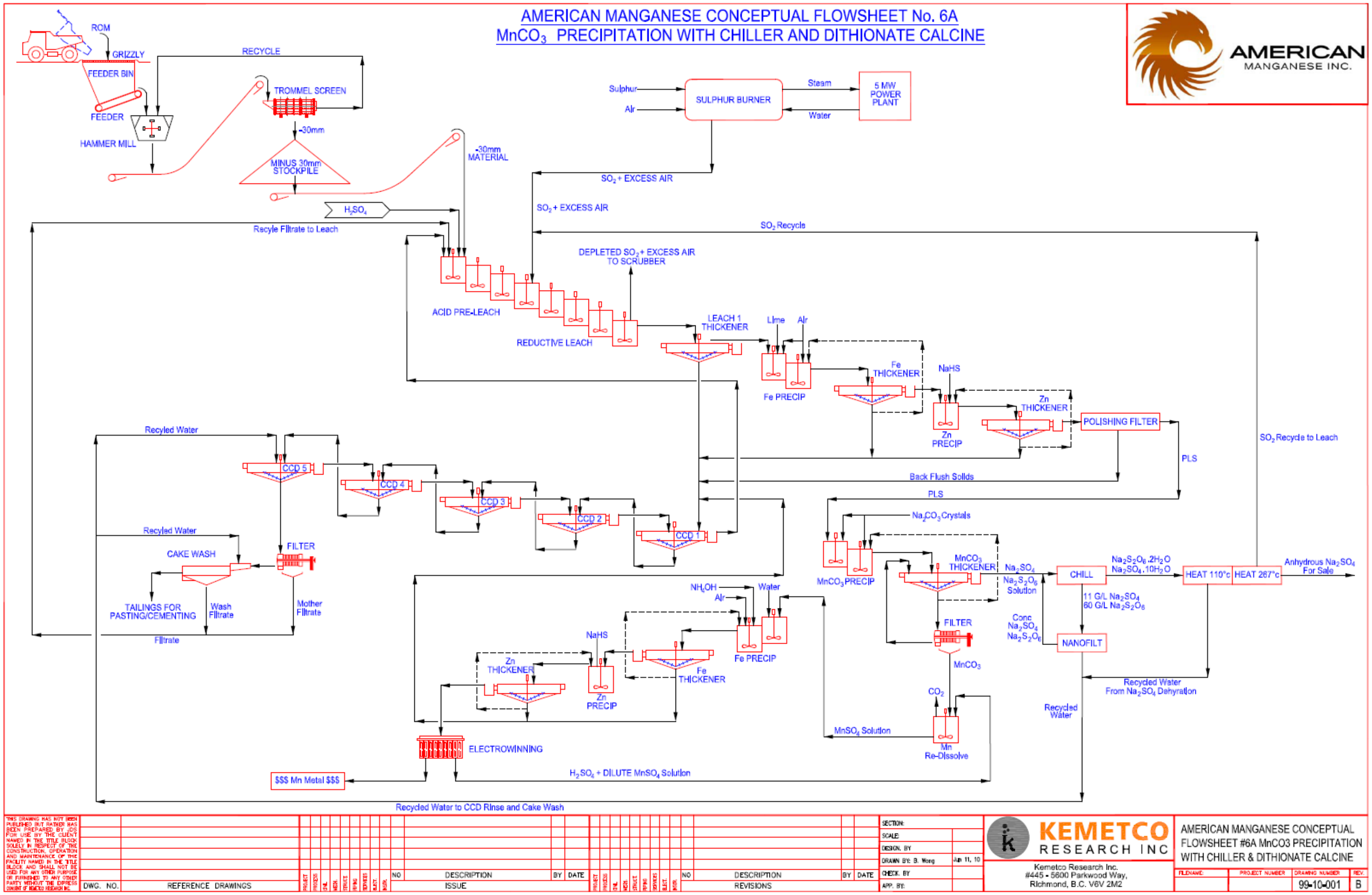

2.2 ALTERNATIVE PROCESS FLOWSHEET WITH BIORECTOR TO RECOVER SO_2, ENERGY AND $NaHCO_3$

An alternative process scheme that uses a proprietary bioreactor to destroy dithionates, and recover SO_2, energy and sodium bicarbonate ($NaHCO_3$) was tested. The alternative flowsheet incorporating this process scheme is shown in Figure 3. While mass and energy balances have not been conducted during this preliminary work, testing of the bioreactor has shown that biological reduction of $Na_2S_2O_6$ can be achieved at a significantly higher rate than biological reduction of Na_2SO_4.

The treatment strategy in the alternative conceptual flowsheet follows the same steps in the main flowsheet described in Section 2.1, except with the following differences:

Carbonate/Bicarbonate Precipitation

Manganese is separated from the PLS by precipitation of solid $MnCO_3$. This is achieved by mixing sodium carbonate and biologically generated sodium bicarbonate solution with the PLS. Precipitation proceeds according to the following reactions:

$$MnSO_4 + Na_2CO_3 \rightarrow MnCO_3 + Na_2SO_4 \quad (11)$$

$$MnS_2O_6 + Na_2CO_3 \rightarrow MnCO_3 + Na_2S_2O_6 \quad (12)$$

$$MnSO_4 + 2NaHCO_3 \rightarrow MnCO_3 + Na_2SO_4 + H_2O + CO_2 \quad (13)$$

$$MnS_2O_6 + 2NaHCO_3 \rightarrow MnCO_3 + Na_2S_2O_6 + H_2O + CO_2 \quad (14)$$

As in the main flowsheet, the solid $MnCO_3$ is separated from the Na_2SO_4 and $Na_2S_2O_6$ by product solution with a thickener. The wet $MnCO_3$ containing underflow is then dewatered in a filtration system and rinsed producing a clean $MnCO_3$ intermediate product for feed into the electrowinning circuit.

Destruction of $Na_2S_2O_6$, Recovery of SO_2, Energy and $NaHCO_3$

The solution by-product produced after precipitation of $MnCO_3$ will contain a mixture of Na_2SO_4 and $Na_2S_2O_6$ dissolved in water. The solution containing Na_2SO_4 and $Na_2S_2O_6$ is fed into the bioreactor with carbon monoxide (CO) and hydrogen gas (H_2) added as an energy source for the bacteria. The net reaction in the bioreactor is as follows:

$$Na_2S_2O_6 + 2CO + 5H_2 \rightarrow 2H_2S + 2NaHCO_3 + 2H_2O \quad (15)$$

The bacteria have been shown to selectively consume $Na_2S_2O_6$ over Na_2SO_4. As such, when $Na_2S_2O_6$ is present, Na_2SO_4 remains mostly unchanged.

In concept, the H_2S generated by the bioreactor can be burned to produce energy and recover SO_2 to be recycled back to the leach. The $NaHCO_3$ bioreactor product will remain mixed with the Na_2SO_4 solution. The solution product from the bioreactor can be fed into the chiller to crystallize $Na_2SO_4{\cdot}10H_2O$ as in the main flowsheet. The mother solution will contain a mixture of dilute Na_2SO_4 and $NaHCO_3$. Separation of the Na_2SO_4 from the $NaHCO_3$ can be achieved with nanofiltration using a membrane that is designed to separate monovalent anions (i.e. HCO_3^-) from divalent anions (i.e. SO_4^{2-}). The concentrate from nanofiltration will contain Na_2SO_4 which can be recycled back to the chiller. The permeate from the nanofiltration unit will contain $NaHCO_3$ solution, which can be fed into reverse osmosis (RO). The concentrate from RO will contain a concentrated $NaHCO_3$ solution which can be recycled back to $MnCO_3$ precipitation. The RO permeate will consist of clean water which can be used to rinse the tailings and be reused in the leaching process.

Figure 3:
American Manganese Alternative Conceptual Flowsheet with Bioreactor

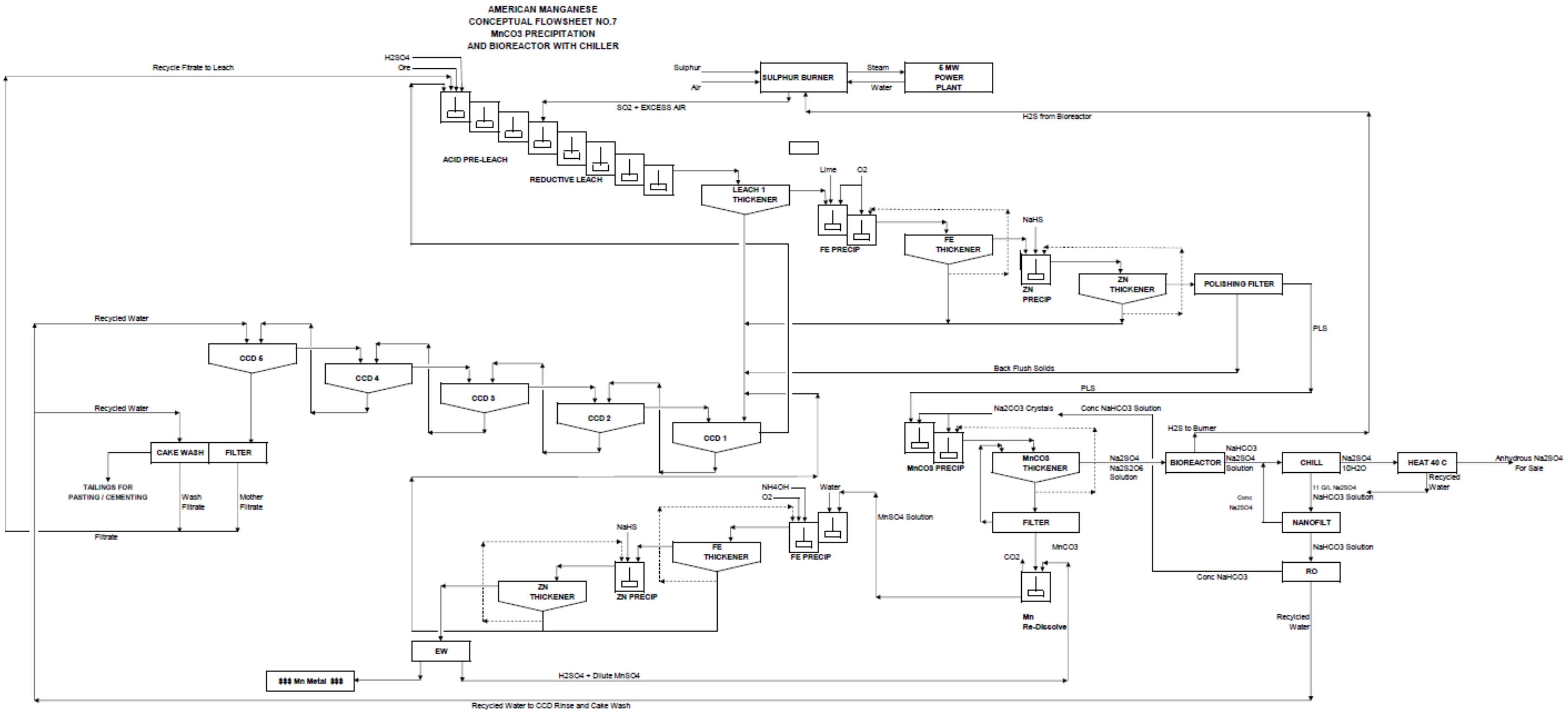

2.3 OTHER PRODUCTS POSSIBLE FROM THE AMERICAN MANGANESE PROCESS

This report focuses on the production of electrolytic manganese metal. Ferromanganese and electrolytic manganese dioxide can be produced with slight modifications to the flowsheets. Production of these alternative products will be briefly described.

2.3.1 Ferromanganese

Lai et al describes a process to make ferromanganese from a $MnCO_3$ starting material[11]. The first step involves decomposition of the $MnCO_3$ by heating to 1000 °C according to the following reaction:

$$MnCO_3 \rightarrow MnO + CO_2 \qquad (16)$$

The MnO is then pelletized with FeO by sintering in a travelling grate rotary kiln. The sintered product is hard spheres (9.5 mm to 15.9 mm) of sintered MnO-FeO. The sinter is a suitable feed to a ferromanganese blast furnace. In the blast furnace, sinter, coke, and limestone are charged, and the sinter reduced at 1550 to 1700 °C to yield metallic ferromanganese.

2.3.2 Electrolytic Manganese Dioxide (EMD)

Electrolytic manganese dioxide (MnO_2) is produced in an undivided electrowinning cell. $MnCO_3$ is dissolved with recycled electrolyte (containing dilute $MnSO_4$ and H_2SO_4) according to the following reaction:

$$MnCO_3 + H_2SO_4 \rightarrow MnSO_4 + H_2O + CO_2 \qquad (17)$$

The $MnSO_4$ solution is fed into the electrowinning cell and MnO_2 is produced on the anode according to the following half cell reaction:

$$Mn^{2+} + 2H_2O \rightarrow MnO_2 + 4H^+ + 2e^- \qquad (18)$$

The half cell reaction on the cathode is as follows:

$$2H_2O + 2e^- \rightarrow H_2 + 2OH^- \qquad (19)$$

The net reaction is as follows:

$$MnSO_4 + 2H_2O \rightarrow MnO_2 + H_2SO_4 + H_2 \qquad (20)$$

The MnO_2 is collected a hard solid sheet on the anode, whereas H_2SO_4 is used to dissolve $MnCO_3$ to replenish Mn in the electrolyte. The H_2 gas is vented.

---

[11] Ralph W. M. Lai, Edwin. L. Owen, "Flotation and Sintering of Synthetic Manganese Carbonate", U.S. Patent #4,274,866, Kennecott Copper Corporation, 1981

3

EXPERIMENTAL RESULTS AND CALCULATIONS

3.1 SAMPLE PREPARATION AND ANALYSIS

The hydrometallurgical work was performed on composite samples from the McGregor Pit area, American Manganese provided in 5 buckets. Each bucket was riffled and split to ensure homogeneity and representative samples were collected, pulverized and sent for whole rock analysis (lithium borate fusion followed by XRF) at ALS Chemex in North Vancouver, Canada. The manganese content varied between 8% and 10.6%, while the iron content was constant at 2.3%. A complete analysis of the samples is given in Table 3. Check assays were performed at ACME (Global Discovery Labs) and Assayers Canada in Vancouver, Canada, by whole rock analysis and four acid digestion / ICP, respectively (data provided in Table 4). The whole rock analysis method gave consistent results, with ALS Chemex yielding slightly higher results. The four acid digestion method reported significantly lower manganese grades, indicating incomplete digestion.

The ore sample with the highest manganese grade (bucket R4) was chosen for most of the subsequent hydrometallurgical scoping work.

Previous reports produced by Mountain States R&D International Inc. in Vail, Arizona, USA and PRA – Inspectorate, in Richmond, BC, Canada revealed that the ore is friable and mechanical agitation during slurrying produces significant amounts of fines that impede filtering and/or settling. The fine material, associated with clay and silt was believed contain little or no manganese, and removing the fine particles prior to leaching would lead to minor manganese losses. To investigate this hypothesis, a particle size analysis was performed on a representative sample weighing approx 1.5 kg removed from bucket R3. The various particle size fractions were then analyzed to determine whether manganese concentrates or not in the material with PS > 2 mm (10 mesh), as initially believed. The particle size analysis and the corresponding manganese assay for each of the particle size fractions are tabulated in Table 5. As seen in Table 5, the material with particle size larger than 2 mm contained more than 9.6% Mn, the manganese content dropping as the particle size decreased. However, even for the fraction with particle size below 60 mesh, the manganese content was still relatively high (6.5-6.8%) and the removal of the < 60 mesh fraction would mean losing about 18% of the total manganese content.

Table 3:
Whole rock analysis of American Manganese composite samples from McGregor area

Sample no	SiO2	TiO2	Al2O3	Fe	Mn	MgO	CaO	Na2O	K2O	P2O5	Ba(F)
(Bucket)	%	%	%	%		%	%	%	%	%	%
R1	48.8	0.4	10.9	2.3	10.6	0.9	4.4	1.6	4.5	0.1	1.7
R2	50.5	0.4	11.3	2.3	9.1	1.0	3.6	1.7	4.6	0.1	1.5
R3	53.7	0.4	11.7	2.3	8.1	1.0	2.7	1.8	4.7	0.1	1.4
R4	51.2	0.4	11.2	2.2	10.5	0.9	3.0	1.7	4.7	0.1	1.7
R5	51.9	0.4	11.4	2.3	9.1	1.0	2.9	1.6	4.7	0.1	1.5

Table 4:
Comparative assays using whole rock analysis and four acid digestion/ICP

	Global Discovery Labs (whole rock analysis)	ALS Chemex (whole rock analysis)	Assayers Canada (Four acid digestion/ICP)
Mn (%)	10.3	10.5	6.8%

Table 5:
Particle size – manganese assay correlation for American Manganese composite

Particle Size		Weight	Indiv. retained	Cum. retained	Mn assay	Mn weight	Cumm Mn	% Mn
Mesh	Diameter(mm)	g	%	%	%	g	g	
x	9.5	181	13	13	9.9	17.8	17.8	15
x	6.3	235	17	30	10.2	23.8	41.6	20
10	2	290	21	52	9.6	27.7	69.4	24
16	1	85	6	58	9.1	7.8	77.1	7
32	0.5	149	11	69	7.1	10.6	87.7	9
60	0.251	121	9	77	6.5	7.8	95.5	7
<60	<0.251	308	23	100	6.8	20.9	116.4	18
Total		1368	100			113.6		100

3.2 SULPHUR BURNING

3.2.1 Description of Operation

The SO_2 required for reductive leaching is generated by the burning of sulphur. It is important to note that sulphur combusted with air produces dilute SO_2 combined with nitrogen (N_2). While leaching test work was conducted with both pure SO_2 and dilute SO_2 mixed with N_2 to simulate a combustion gas, experiments with dilute SO_2 would be more realistic in practice.

The operation of a sulphur burner involves melting elemental sulphur by heating to above 115 °C. The liquid sulphur is atomized with dry air and combusted in a combustion chamber. Liquid sulphur is delivered in a jacketed tube heated with steam to prevent solidification. Excess air is used in the combustion process to prevent carry-over of sulphur which can coat and foul equipment subsequent to the combustion chamber. Residual sulphur trioxide (SO_3) gas needs to be scrubbed with an acid absorber. The exhaust gas from the sulphur burner can be heat exchanged to produce steam for power generation. To prevent corrosion in the heat exchanger tubes, it is important not to decrease the temperature to below 150 °C. To provide a margin of safety, heat exchanging the exhaust gas to 400 °C would be a practical temperature.

3.2.2 Stoichiometry and Mass Balance

The combustion of sulphur with 20% excess air would proceed according to the following reaction:

$$S + 1.2O_2 + 4.5N_2 \rightarrow SO_2 + 0.2O_2 + 4.5N_2 \qquad (21)$$

According to Reaction 21, the molar ratio of the SO_2 in the exhaust gas would be 17.5%.

With the basis of 140 metric tonnes per day of Mn production and assuming that 10% molar excess SO_2 is used in the leach, approximately 91 metric tonnes per day of elemental sulphur will be required to feed the process.

3.2.3 Heat and Power Generation Calculations

In order to calculate the energy produced by the burning of sulphur, the thermodynamic data provided in Table 6 is required[12].

Table 6:
Thermodynamic Data for Sulphur Burning Calculations[12]

Heating Value of S (KJ/mole)	296.81
$C_{p\,[SO2\,gas]}$ (cal/mol·K)	$7.70 + 0.00530T - 0.00000083T^2$
$C_{p\,[O2\,gas]}$ (cal/mol·K)	$8.27 + 0.000258T - 187700/T^2$
$C_{p\,[N2\,gas]}$ (cal/mol·K)	$6.50 + 0.00100T$

The first step in determining the usable energy from the combustion of sulphur is to determine the adiabatic flame temperature. This is determined by balancing the heat generated by the full heating value of sulphur with the heat transferred to the exhaust gas (from an ambient temperature starting point).

The heat content in the exhaust gas can be calculated by integrating the specific heat with respect to temperature for each individual gas in the exhaust and multiplying by the molar amount of each gas. The formula for this calculation is as follows:

$$\text{Heat in Exhaust} = \Sigma\, n_i \int C_p\, dT \qquad (22)$$

Where n_i = number of moles of each gas in the exhaust

The integrated specific heats for each component of exhaust gas are provided in Table 7.

---

[12] Perry's Chemical Engineers Handbook, 8th Edition, Mcgraw-Hill, 2008, pp 1.237 – 1.298 & 2.156 – 2.163

Table 7:
Calculation of Energy in Exhaust Gas (Cal/mol); T (^{o}K)

$\int_{T_{initial}}^{T_{final}} C_{pSO_2}\,dT$	$=\left[7.70T_{final}+\left(\frac{0.00530}{2}\right)T_{final}^{2}-\left(\frac{0.00000083}{3}\right)T_{final}^{3}\right]-\left[7.70T_{initial}+\left(\frac{0.00530}{2}\right)T_{initial}^{2}-\left(\frac{0.00000083}{3}\right)T_{initial}^{3}\right]$
$\int_{T_{initial}}^{T_{final}} C_{pO_2}\,dT$	$=\left[8.27T_{final}+\left(\frac{0.000258}{2}\right)T_{final}^{2}+\left(\frac{187700}{T_{final}}\right)\right]-\left[8.27T_{initial}+\left(\frac{0.000258}{2}\right)T_{initial}^{2}+\left(\frac{187700}{T_{initial}}\right)\right]$
$\int_{T_{initial}}^{T_{final}} C_{pN_2}\,dT$	$=\left[6.50T_{final}+\left(\frac{0.00100}{2}\right)T_{final}^{2}\right]-\left[6.50T_{initial}+\left(\frac{0.00100}{2}\right)T_{initial}^{2}\right]$

By burning elemental sulphur with 20% excess air from an ambient temperature of 25 ^{o}C, the adiabatic flame temperature was calculated to be 1509 ^{o}C.

Burning 91 metric tonnes per day of sulphur with 20% excess air and heat exchanging the exhaust gas to 400 ^{o}C, will produce 20 tonnes per hour of steam at 45 bar pressure. Assuming 50% efficiency for the condensing turbine, approximately 5 MW of continuous electrical power will be generated.

Depending on the temperature requirements of the process, a further 2.2 MW of low grade heat is available in the exhaust gas for thermal applications ranging from 400 ^{o}C to 25 ^{o}C.

3.3 REDUCTIVE LEACHING WITH SO_2

There are a number of key aspects of the hydrometallurgical processing of lower grade Mn resources that have to be considered. They are:

- The resources in the Artillery Peak, Arizona region are generally less than 7% manganese by weight and are not amenable to upgrading by flotation and/or gravity separation.
- High content of silt and clay are a significant impediment in heap leaching, as the percolating rates are very low.
- The friable nature of the material, in association with the silt and clay elements make the solid/liquid separation and washing challenging.

- To improve the settling properties and reduce the grinding cost, leaching of coarse particle size resource is desired.
- The presence of Mn^{4+} requires the use of a reducing agent such as SO_2, to convert the insoluble Mn^{4+} to the soluble Mn^{2+} form.
- The manganese extraction with SO_2 is associated with formation of dithionates.
- Achieving maximum manganese extraction into solution is desirable.
- Producing a pure manganese sulphate solution with Mn concentration above 40g/L is required to produce EMM.
- High acid consumption should be avoided.

The Artillery Peak mineralization consists of a mixture of manganese oxides, among which the most important are pyrolusite (MnO_2), psilomelane ($(BaH_2O)_2Mn_5O_{10}$) and wad. As shown in the E-pH diagram for the manganese – water system (Figure 4), reducing Mn^{4+} and Mn^{3+} oxides to Mn^{2+} with a reducing agent such as SO_2 dissolved in water would solubilise the Mn[13].

---

[13] Atlas of Electrochemical Equilibria in Aqueous Solutions, Marcel Pourbaix, Nace Publishing, 1974.

Figure 4:
E-pH Diagram for the Manganese - Water System[13].

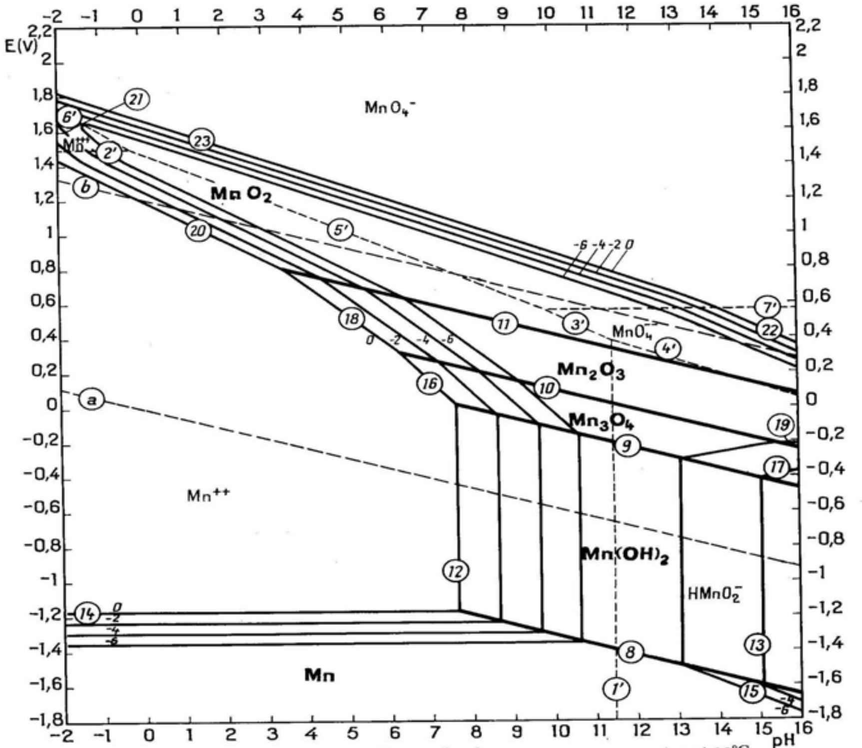

FIG. 1. Potential–pH equilibrium diagram for the system manganese–water, at 25°C. [Considering β-MnO_2 (pyrolusite).]

The manganese extraction with sulphurous acid (SO_2 dissolved in water) results in a solution containing a mixture of manganese sulphate ($MnSO_4$) and manganese dithionate (MnS_2O_6). Minor impurities such as iron, calcium, aluminum, arsenic and zinc are also leached in solution. The presence of dithionates during manganese electrodeposition is not desirable, as it has detrimental influence on the quality of the electrolytic manganese metal product. Some of the main reactions assumed to take place during the reduction leaching are listed below:

$MnO_2 + SO_2 \rightarrow MnSO_4$ (23)

$MnO_2 + 2SO_2 \rightarrow Mn_2S_2O_6$ (24)

$Mn_2O_3 + H_2SO_4 + SO_2 \rightarrow 2MnSO_4 + H_2O$ (25)

$Mn_2O_3 + H_2SO_4 + 2SO_2 \rightarrow MnSO_4 + MnS_2O_6 + H_2O$ (26)

$Mn_3O_4 + H_2SO_4 + SO2 \rightarrow 3MnSO_4 + MnS_2O_6 + 2H_2O$ (27)

The formation and build up of dithionates in the process liquor was one reason why a leach system with SO_2 was never employed on commercial scale. The presence of dithionates during the deposition EMM or EMD was reported to lead to H_2S release and can affect the quality and purity of the product[14].

Preliminary tests performed with sulphuric acid alone yielded no manganese extraction, confirming that no M^{2+} species are present in the Artillery Peak resource.

3.3.1 Factors Influencing the Manganese Extraction and Dithionate Formation

Factors influencing leaching were studied utilizing a full factorial experimental design, with particle size, pulp density, SO_2 concentration and H_2SO_4, as main factors and manganese extraction and dithionate concentration in the pregnant solution as responses. Stoichiometry was not considered an independent variable, as it depends on both SO_2 concentration and pulp density and cannot be varied without changing one of the main factors

The effect of temperature was not investigated, however, the leaching reaction was observed to be exothermic. Although a decrease in temperature would be beneficial, both for the sulphur dioxide dissolution in water and for the manganese extraction, this option was not investigated.

For the purpose of the experimental design, a minimum, symbolized by (-) and maximum, symbolized by (+) were chosen for each of the effects investigated, as tabulated in Table 8. As seen in Table 8, the maximum pulp density used was about 27%, while the minimum was approx 10%. The tests were performed using particle (PS_{80}) of 6 and respectively 70 mesh (3.36 mm and 210 µm), while the sulphuric acid concentration was 0.02 and 0.1M, respectively. The average manganese content of the 6 and 70 mesh samples were around 10.2% and 7.1%, respectively.

The sulphurous acid solutions were obtained by sparging pure SO_2 gas from an SO_2 gas cylinder in DI water, to achieve a stock solution with the maximum concentration of 6% by weight. The minimum SO_2 concentration tested, 2.4% by weight, was obtained by diluting the stock solution with DI water.

The tests were performed in sealed bottles that were rolled to ensure continuous mixing of the slurry and samples were removed at various time intervals. The tests were terminated after 20 hours and the solid residues washed and sent out for analysis by fusion/XRD. The manganese concentration in solution analysis was analyzed by ICP. A direct method for dithionate analysis was developed in house, using Dionex 4500i ion chromatography with conductivity detector. The dithionate ($S_2O_6^{2-}$) was determined with a 4x50 mm Dionex AG4A-SC column and 2g/L Na_2CO_3 eluent at 1 mL/min, while the sulphates were determined with an AS4A column and a Na_2CO_3/$NaHCO_3$ eluent at 2 mL/min. The initial SO_2 concentration in aqueous solutions was determined by iodometric titrations

The experimental conditions, along with the resulting manganese extractions calculated based on the solid residue analysis by fusion/ XRF are provided in Table 8.

Increasing the particle size from 70 mesh to 6 mesh decreased only slightly the manganese extraction when using the maximum SO_2 concentration of 6 wt%. The pulp density and the

---

[14] Christopher Ward, “Hydrometallurgical Processing of Manganese Containing Materials”, PCT Patent Application #WO 2004/033738 A1, HITECH ENERGY LIMITED, 2004.

sulphurous acid concentration (stoichiometry) exhibited the largest effect on the final manganese extraction, both the kinetics and the manganese extractions were improved when working with 10% pulp density and 6 wt% SO_2 solution. SO_2 concentration became an important factor especially when working at high pulp density, as seen in Figure 5. Similarly, the sulphuric acid concentration had no effect at low pulp density, but became relevant high pulp density (Figure 6). Even more, manganese extraction of 98% was achieved at 10% pulp density and 6% SO_2 , without any sulphuric acid addition. Low SO_2 concentration correlated with large particle size had a detrimental effect on the manganese extractions, as well on the reaction kinetics.

The dithionate concentration was mainly influenced by pulp density and SO_2 concentration, as the availability of both MnO_2 and SO_2 promoted the formation of dithionates. The presence of excess MnO_2 did not decrease the dithionate concentration dramatically. As seen in Table 8, dithionate concentrations higher than 15g/L were observed even at $[SO_2]/[Mn]$ molar ratio of 0.54. Another factor influencing the dithionate concentration was the sulphuric acid concentration. Higher sulphuric acid concentrations contribute to the dithionate destruction. For example, bottle roll tests performed on 70 mesh samples, with 6% wt SO_2, at 10% pulp density, yielded 12.7 g/L dithionate concentration when 0.1 M sulphuric acid was used, 25.3 g/L when 0.02M sulphuric acid was used and close to 30g/L when using no sulphuric acid.

Figure 5:
The Effect of Pulp Density (% wt) and SO_2 conc. (%wt) on Mn extraction (%)

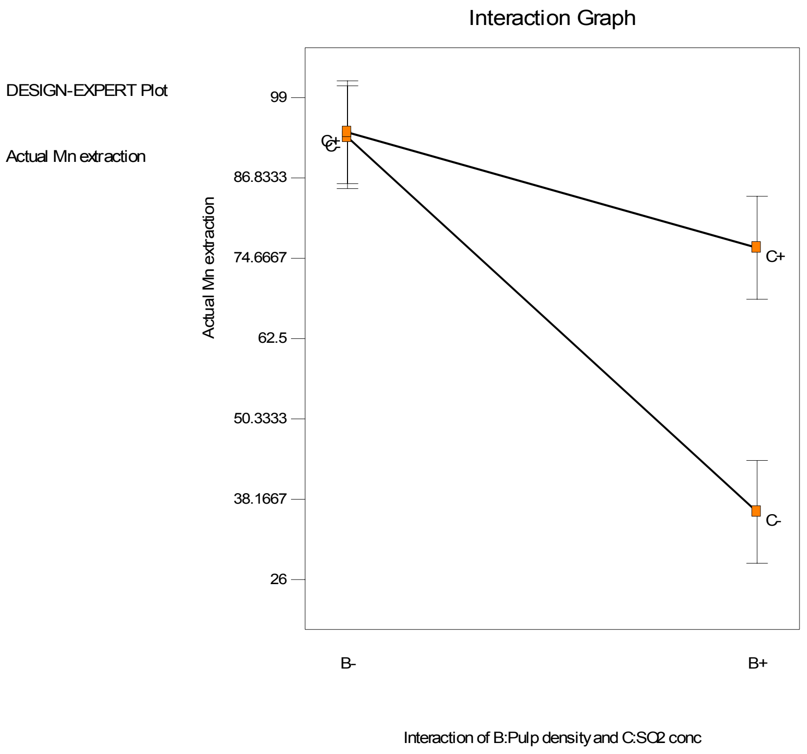

Table 8:
Experimental Design Test Conditions and Results

Run	PS	Pulp density	SO2 conc	H2SO4 conc	PS	Pulp density	SO2 conc	H2SO4 conc	[SO2]/[Mn]	pH	Mn	Mn extr (20h)	$S_2O_6^{2-}$ conc (20h)
	mesh	(wt%)	(wt%)	(M)	mesh	(wt%)	(wt%)	(M)			g/L	(%)	(g/L)
1	6	10%	6	0.02	+	-	+	-	4.54	1.4	11.0	96%	25.3
2	70	10%	6	0.1	-	-	+	+	6.53	1.2	7.7	94%	18.7
3	6	27%	6	0.1	+	+	+	+	1.34	1.6	36.7	95%	69.2
4	70	27%	2.4	0.1	-	+	-	+	0.77	6.6	11.9	47%	30.2
5	6	27%	2.4	0.02	+	+	-	-	0.54	6.6	8.6	26%	24.8
6	70	10%	2.4	0.02	-	-	-	-	2.61	2.3	8.1	96%	21.9
7	70	27%	6	0.02	-	+	+	-	1.93	6.4	17.5	57%	65.6
8	6	10%	2.4	0.1	+	-	-	+	1.81	1.3	9.5	93%	17.5
9	70	10%	6	0.02	-	-	+	-	6.53	1.1	8.2	97%	21.8
10	6	10%	2.4	0.02	+	-	-	-	1.81	1.5	10.0	84%	19.1
11	70	27%	6	0.1	-	+	+	+	1.93	1.1	25.3	97%	56.4
12	6	27%	6	0.02	+	+	+	-	1.34	4.4	19.6	56%	47.7
13	70	27%	2.4	0.02	-	+	-	-	0.77	5.7	9.9	33%	27.6
14	6	27%	2.4	0.1	+	+	-	+	0.54	1.1	11.5	39%	16.4
15	6	10%	6	0.1	+	-	+	+	4.54	0.8	9.3	88%	12.7
16	70	10%	2.4	0.1	-	-	-	+	2.61	0.8	8.2	99%	19.8

Figure 6:
Effect of Pulp Density (%wt) and H_2SO_4 Concentration (M) on the Mn Extraction (%)

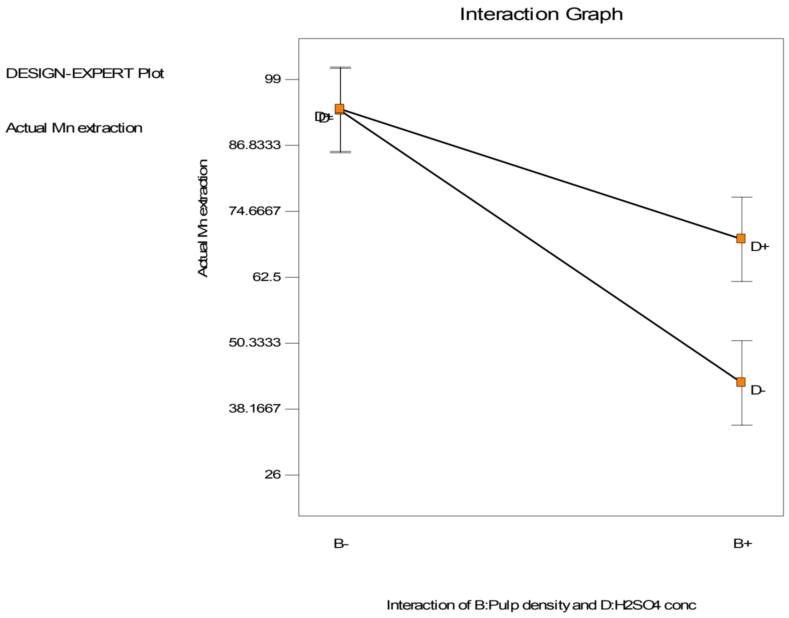

Figure 7:
Variation of Manganese Extraction as a Function of Pulp Density (% wt) and SO_2 Concentration (% wt)

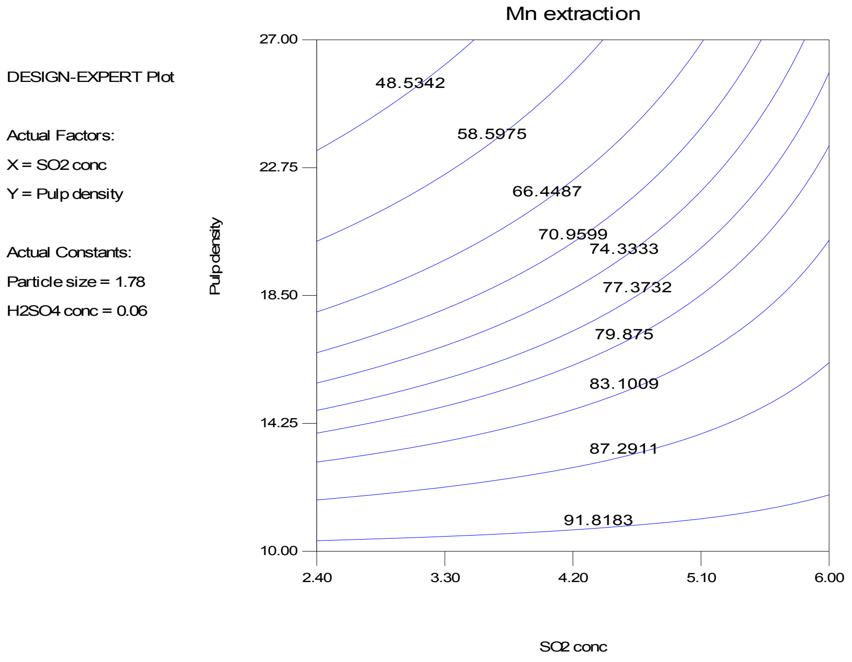

Figure 8:
Variation of Mn Extraction as a Function of Particle Size (mm) and SO_2 Concentration (% by weight)

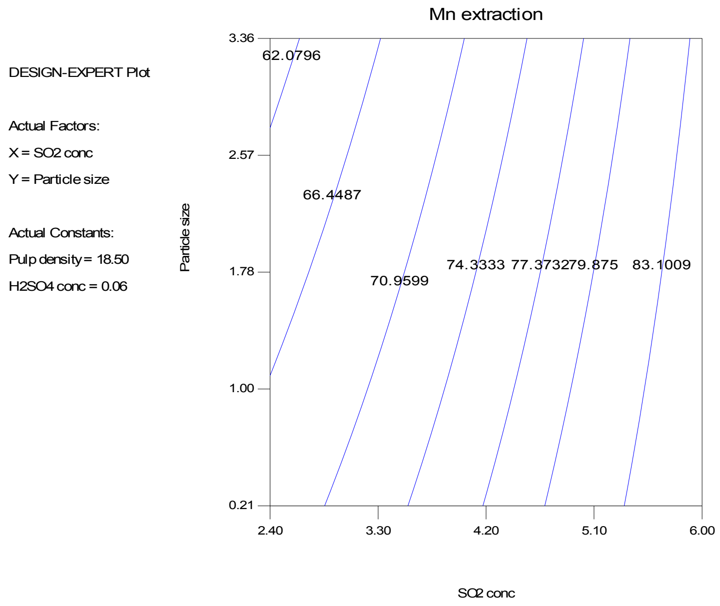

Figure 9:
Variation of Dithionate Concentration (g/L) as a Function of SO_2 Concentration (% wt) and Pulp Density (%wt)

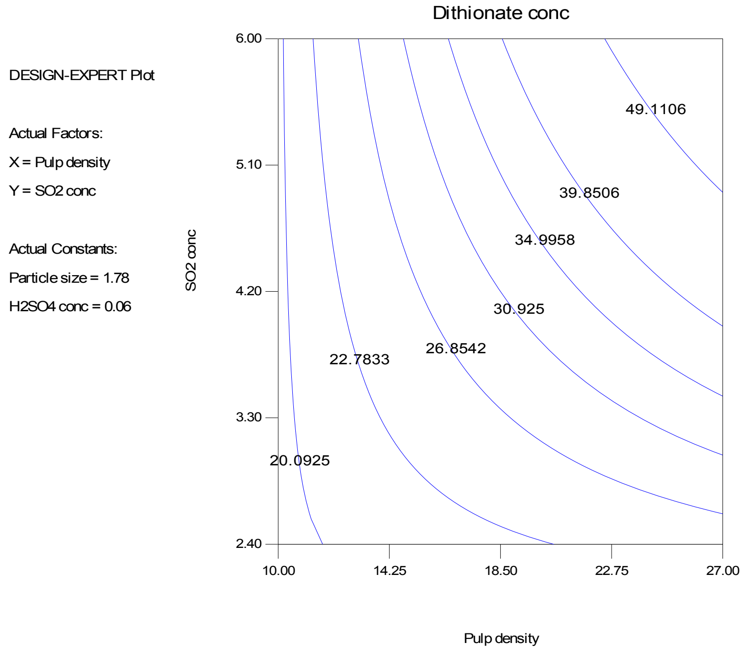

3.3.2 Stirred Tank Counter Current Leaching with Concentrated SO_2

The concept of counter current leaching as a method of destroying the dithionates was investigated by performing a 3 stage scoping test. The first stage leach test was performed in magnetically stirred reactor at 10% pulp density, on the manganese ore with PS < 100µm. The lixiviant contained 0.05M sulphuric acid and approx 6% SO_2. After two hours, the slurry was filtered and the filtrate was used in the 2nd stage to leach a fresh ore sample. Similarly, the pregnant solution from the 2nd stage was used to leach a fresh ore sample in the 3rd stage. The tailings from each of the three tests were washed and sent for analysis.

The test conditions and the results are tabulated in Table 9. As the first stage was performed with excess SO_2, complete manganese extraction was attained in the first two hours. In the second stage, the residual SO_2 was consumed by the fresh ore, increasing the manganese concentration from 11g/L at the end of the first stage, to 16 g/L at the end of the second stage. No additional manganese was extracted during the third stage and even significant MnO_2 excess did not result in dithionate destruction. Probably due to the neutral pH, the residual sulphites reacted with the pyrolusite to produce additional dithionates.

However, besides facilitating complete SO_2 consumption, the counter current leaching also allows the economical utilization of the ore alkalinity to purify the pregnant solution. As seen in Table 9, at the end of the first stage, some of the main impurities were Fe (269 ppm), Al (102 ppm) and As (42 ppm). The increase in pH from 1.2 to 2 lead to a significant reduction in all three impurities, while at pH 6.3 the pregnant solution contained less than 1 ppm Fe, Al and As.

Table 9:
Counter Current Leaching – Conditions and Results

Sample	Time	Sample vol	Volume	Wt solids	pHf	Free SO2%	$S_2O_6^{2-}$	Mn	Net Mn	Fe	Al	Ca	Cu	K	Zn	As	Mn	Mn extr	Fe	Fe extr
	(min)	mL	mL	(g)			g/L	ppm	ppm	ppm	ppm	ppm	ppm	ppm	ppm	ppm	(g)	(%)	(g)	(%)
1st stage				100																
1	5	10	900			6%		11174		244	60.9	1941	5.30	252	34.3	40.6	10.06	98%	0.22	10%
2	10	10	890					11347		253	66.7	1698	5.33	243	31.1	42.8	10.21	99%	0.23	10%
3	20	10	880					11307		258	70.9	1559	5.39	235	31.0	44.6	10.17	99%	0.23	10%
4	30	10	870					11277		258	72.1	1469	5.44	233	30.9	41.8	10.15	99%	0.22	10%
5	60	10	860					11172		261	77.3	1514	5.29	233	30.9	43.0	10.06	98%	0.22	10%
6	120	10	850		1.2	1.3%	22	11413		269	102	1724	5.55	249	31.9	42.0	10.26	100%	0.23	11%
2nd stage				83																
1	5	10	745					12455	1042	198	42.0	1562	6.02	231	39.6	42.3	0.78	9%		
2	10	10	735					14176	2764	95.5	42.3	1246	5.70	238	40.2	38.7	2.04	24%		
3	20	10	725					14667	3254	87.6	38.7	1225	4.60	221	40.5	33.7	2.40	28%		
4	30	10	715					15008	3595	67.8	33.7	1289	3.98	214	40.9	32.0	2.64	30%		
5	60	10	705					16317	4905	15.4	32.0	1239	1.85	218	40.6	17.7	3.53	41%		
6	120	10	695		2.0	0.3%	26	16825	5413	4.18	17.7	1250	1.37	223	40.0	9.79	3.92	45%		
3rd stage				70																
6	120	10	595		6.3	-	33	16206		<1.	<1.	1479	<1.	248	21	<1.				

3.3.3 Stirred Tank with Dilute SO_2

Following a meeting with Noram Engineering and Constructors Ltd. of Vancouver, Canada, we were advised to perform additional leaching work using a gas mixture containing 14-16 vol% SO_2 and 84-86% N_2, as producing SO_2 by burning sulphur is practical only when using air as the oxidant. As a result, a series of additional stirred tank tests on ore samples of various particle sizes were performed with a SO_2/N_2 mixture, using the experimental set-up presented in Figure 10. The pulp density and sulphuric acid concentrations were maintained at 10% and 0.05M, respectively and the mixing of the slurry was achieved using a magnetic stirrer. The mixture of SO_2 (50 mL /min) and N_2 (270 mL/min) was sparged directly into the slurry. The excess SO_2 was scrubbed in 3M NaOH solution, and the extraction tests were considered terminated when the SO_2 concentration in the scrub solution reached approx 1g/L. The manganese extraction dropped from 94% when leaching samples characterized by PS <100 mesh (<0.15 mm), to approx 73% when the PS increased to 6 mesh (3.36 mm). The manganese extraction was reduced to as low as 55% at particle sizes as large as 3 mesh (6.7 mm). Because the ore is friable and breaks down during agitation, longer retention times yielded better manganese extractions. However, the magnetic agitation was not strong enough to reduce the particle size enough for complete manganese extraction.

Figure 10:
Experimental Set-up for Manganese Extraction with SO_2/N_2 Mixture

The stirred tank tests performed so far, confirmed that leaching of coarse samples, with dilute SO_2 gas is technically viable and milling prior to the leaching stage is not obligatory. Nevertheless, complete manganese extractions can only be achieved slowly, as the material breaks down to particle size below 70 mesh.

A subsequent test was performed at 40% pulp density, on a coarse sample containing more than 35wt% particles larger than 9.5 mm. To accelerate the manganese extraction, the slurry agitation was attained using an overhead mixer (Figure 11). The manganese extraction increased with the decrease in the particle size, from 17% after 1 hour, to 90% after 12 hours.

Figure 11:
Stirred Tank Leaching with SO_2/N_2

3.3.4 Column Leach Test with Dilute SO_2

Under certain circumstances, column leaching can be an alternative to the stirred tank approach, especially because it would circumvent the subsequent solid-liquid separation stage. To assess such leaching method, a column with 5 inch diameter and 6.5 inch height was packed with approx 2 kg manganese ore sample previously screened to be +2mm / -35 mm (Figure 12). 0.5 M sulphuric acid solution was percolated through the column at an initial flow rate of 25 mL/min. The mixture of SO_2 (50 mL/min) and N_2 (250 mL/min) was introduced at the bottom of the column and allowed to move upwards through the ore sample. After only a few minutes it became apparent that the material started to break down quickly, causing the column to plug, so the sulphuric acid flow rate was drastically reduced and eventually stopped. The test was terminated after approx 4 hours and a particle size analysis of the solid residue was performed.

As seen in Table 10, if the initial particle size did not exceed 2 mm, approx 20% of the final residue is characterized by a particle size below 2 mm, more than 10% being below 0.5 mm. The whole rock analysis of the various particle size fractions also revealed that the smaller the particle size, the higher manganese extraction. While the fraction below 0.5 mm had a residual manganese content of 2.6%, the larger particle size fractions (> 6.3 mm) did not show any indication of manganese extraction.

In conclusion, although the column leaching approach has the advantage of eliminating the difficult solid-liquid separation stage, complete manganese extraction requires extended periods of times and the column could easily plug up due to the clay and silt material released during leaching.

Figure 12:
Column Leach Set-up

Table 10:
Ore Sample Characterization Before and After Column Leaching Test

		Feed material			Solid residue		
Mesh	**Diameter**	**Wt**	**Retained**	**Mn**	**Wt**	**Retained**	**Mn**
	mm	**g**	**%**	**%**	**g**	**%**	**%**
x	9.5	500.23	24.99	9.9%	467.8	24.38	10.2%
x	6.3	660.95	33.02	10.2%	456.63	23.80	10.6%
10	2	840.51	41.99	9.6%	540.41	28.17	8.7%
16	1				104.34	5.44	5.3%
32	0.5				104.77	5.46	4.2%
<32	<0.5				244.76	12.76	2.6%
Total		**2001.69**	**100.00**		**1918.71**	**100.00**	

3.4 SOLID LIQUID SEPARATION

As a part of flowsheet development for manganese recovery, a series of settling tests were conducted using fresh leach solutions under a range of possible operating conditions. The objective of this work was to evaluate the effects of common flocculants and to provide sufficient settling data to allow confidence in sizing of thickeners for solid-liquid separation.

3.4.1 Flocculant Screening

On-going optimization of the process stages prior to settling has identified several possible operating conditions for feed particle size and pulp density. To ensure that there is sufficient settling data to cover the range of likely operating conditions, a test matrix was established to evaluate different types and levels of flocculant addition using both coarse and fine feed, and using low and high pulp density in the leach.

The test matrix is shown below:

Table 11:
Settling test matrix

Pulp Density	**10% solids**			**20% solids**		
Grind Size	No floc	Percol 351	Percol E24	No floc	Percol 351	Percol E24
6#	x	5 ppm	5 ppm	x	10 ppm	10 ppm
6#		10 ppm	10 ppm		30 ppm	30 ppm
70#	x	10 ppm	10 ppm	x	30 ppm	30 ppm

In addition to the above 16 tests, one test was added with 70# feed leached at 30% solids. This test used Percol 351 at 10 ppm as a flocculant. A further test involved decanting the leach solution after one of the above tests (6# feed leached at 10% solids and settled with 5 ppm Percol 351) and re-pulping the settled solids with de-ionized water to conduct another settling test without further flocculant addition. This latter test was to simulate a counter current washing stage in the process circuit.

Each test consisted of production of test feed by carrying out a 1 litre leach using the specified pulp density and size of feed material, followed by transfer of the entire leach pulp to a 1 litre graduated cylinder for settling measurement. If required, flocculant in the specified dosage was added as a pre-mixed 1 g/L solution. The initial slurry level was marked and the covered cylinder was inverted several times to ensure complete mixing, and to give flocs an opportunity to form. The cylinder was the set down and a timer started. As soon as a solid-liquid interface was evident, the level was recorded at short time intervals until settling slowed to the compression phase. The level was then checked and recorded again intermittently over 2-4 hours, and a final level was recorded after 24 hours.

Tests allowed comparison of settling of un-flocculated slurry with different flocculants. While there are many types of flocculant available, keeping the test matrix to a reasonable size required narrowing the choice to a small number of likely options. For this testing one anionic (Percol E24) and one non-ionic (Percol 351) flocculant were chosen. Both are very commonly used in industry, and Percol 351 is known to be used by other manganese operations. The dosages used cover a typical range for low pulp-density slurries.

Data recorded from each test were used to produce settling curves such as those shown in Figure 13. In general, these all showed the classic steep zone settling phase at the start, followed by slow compression settling after the first few minutes.

Figure 13:
Settling curves for 6 mesh feed leach at 10% solids

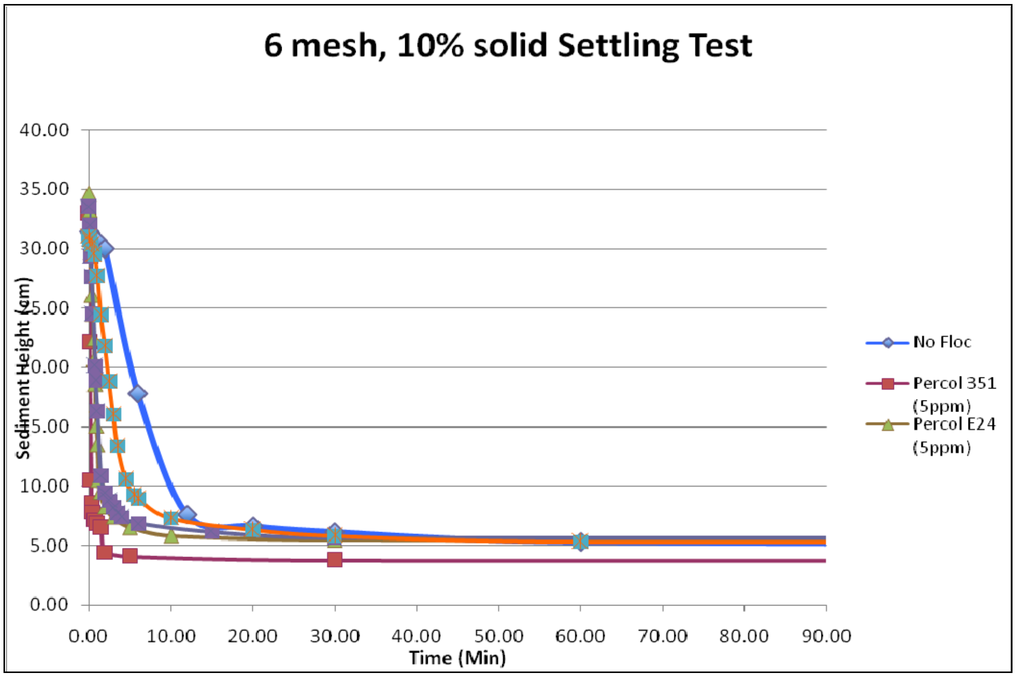

Overall results from all settling tests are summarized in Table 12. For each test a settling rate was obtained from the slope of the zone settling section of the settling curve, expressed in cm/min. The final settled volume after 24 hours allowed the settled density to be calculated, based on an assumed average solid specific gravity of 2.5.

Table 12:
Compiled settling test results

Test #	Feed	Density	Dose (ppm)	Floc	Settling Rate (cm/min)	Final Volume (ml)	Settled Density (% solids)
1	6#	10%		None	3.05	140	50.0
4	70#	10%		None	1.42	180	41.7
9	6#	20%		None	1.37	290	48.8
12	70#	20%		None	0.47	350	42.6
2-wash	6# wash	10%		None	9.66	150	47.6
3	6#	10%	2 ppm	Percol 351	15.17	155	46.5
2	6#	10%	5 ppm	Percol 351	73.44	107	59.9
5	70#	10%	5 ppm	Percol 351	6.65	190	40.0
10	6#	20%	5 ppm	Percol 351	18.29	270	51.3
11	6#	20%	10 ppm	Percol 351	6.44	280	50.0
13	70#	20%	10 ppm	Percol 351	0.63	330	44.4
17	70#	30%	10 ppm	Percol 351	2.40	365	55.0
7	6#	10%	2 ppm	Percol E24	5.04	150	47.6
6	6#	10%	5 ppm	Percol E24	20.64	150	47.6
8	70#	10%	5 ppm	Percol E24	2.23	190	40.0
14	6#	20%	5 ppm	Percol E24	9.57	240	55.6
15	6#	20%	10 ppm	Percol E24	15.05	250	54.1
16	70#	20%	10 ppm	Percol E24	0.68	325	44.9

For comparison purposes, settling rates and final densities were plotted for each flocculant tested, as shown in Figures 14 to 16. Both flocculants provided significant improvements over settling without flocculation in all cases, with the difference being especially dramatic at lower pulp densities.

Interestingly, the relative effectiveness of the two flocculants tested changed with the nature of the test feed. At 10% solids, Percol 351, the non-ionic flocculant, was extremely effective, achieving about 3 times the settling rate of Percol E24, and many times the rate without the use of flocculant. With higher pulp densities, the difference between the two flocculants was less, and the finer material at 20% solids, E24 performed slightly better, although the rate was low for all tests with this feed.

Figure 14:
Settling results without flocculant

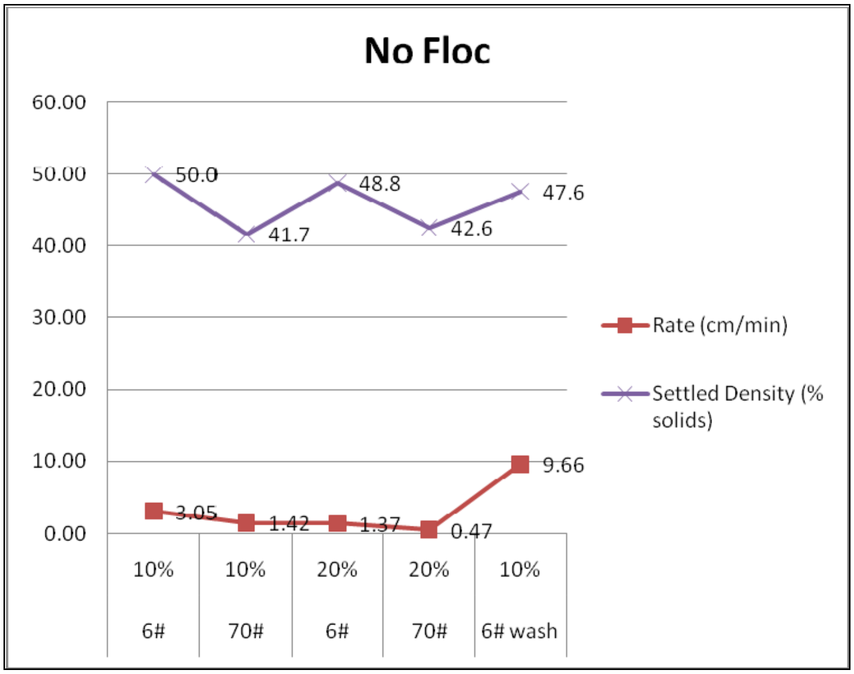

Figure 15:
Settling results with Percol 351

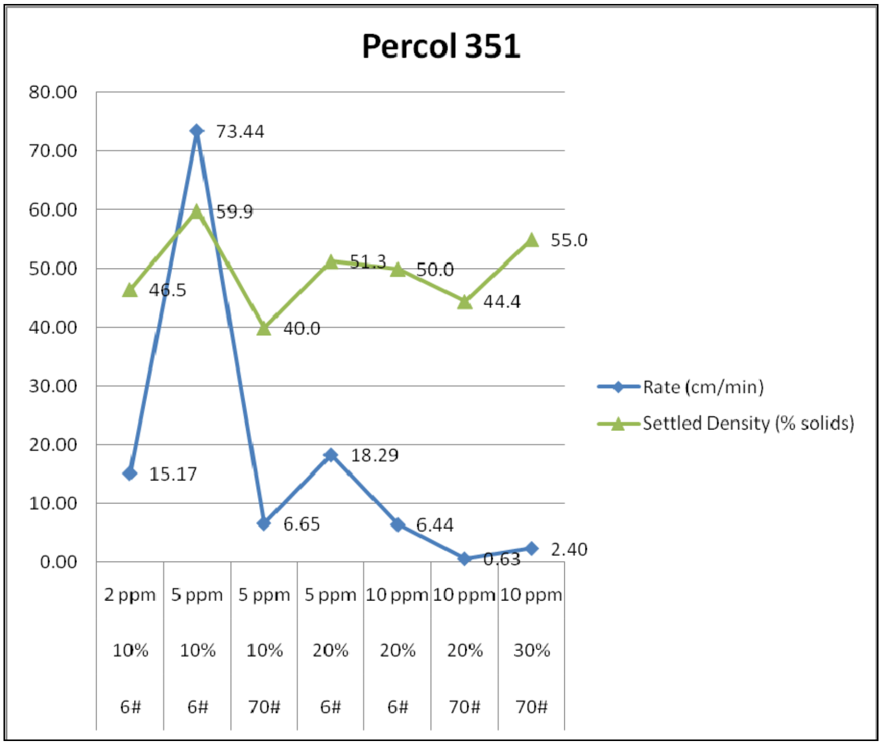

Figure 16:
Settling results with Percol E24

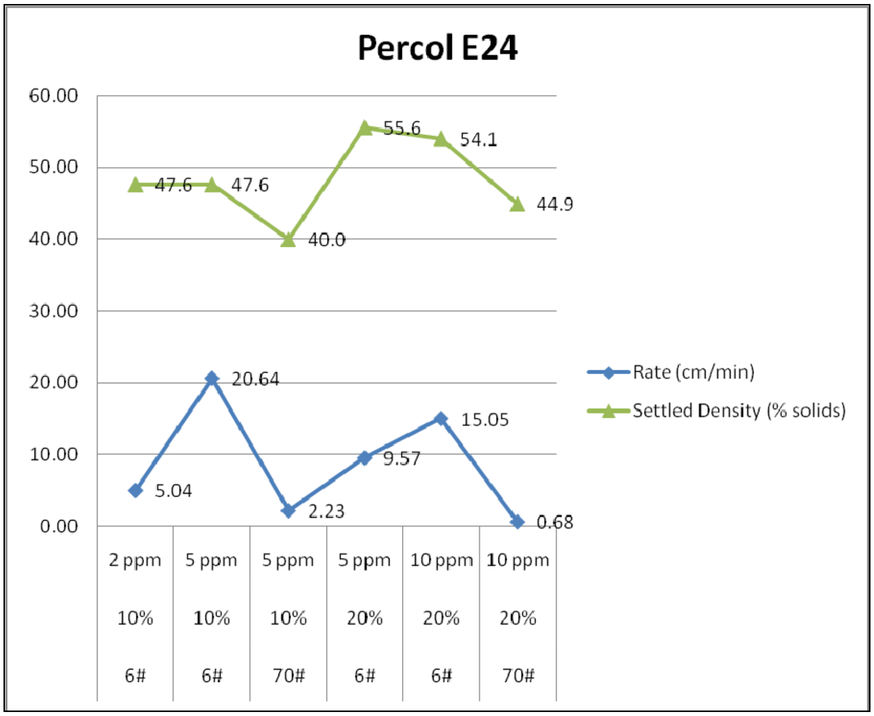

Percol E24 also gave higher final densities than E351 with the higher initial pulp density. Also, at the higher pulp density, E351 appeared to work best at a lower dose, losing effectiveness when the dosage was doubled. E24 however, showed significantly improved results at higher strength.

In conclusion, some very effecting flocculation/settling results were obtained when using low pulp densities. Higher densities, which are more likely to be required for effective process operation, also show significantly improved settling with proper flocculant addition, but this has probably not yet been optimized.

The quantity of fines present is also a very important parameter, and if processing will result in substantial fines generation, then further optimization of settling would also need to focus on fines. When the operating conditions for the leaching have been more defined, additional settling work can be focused on those conditions to minimize the solid-liquid separation equipment requirements.

The best result to date, 73 cm/min at 10% solids using a lower dose of Percol E351 non-ionic focculant. While additional work is required to improve settling rates at higher pulp densities, preliminary design work will focus around the best operating conditions, which consists of lower pulp density and the use of a non-ionic focculant.

3.4.2 Preliminary Leached Ore Thickener and CCD Sizing

Counter current decantation (CCD) thickener circuits are used to recover soluble values in pregnant liquor from leached slurries. The basis of CCD operation is to concentrate suspended solids thereby minimizing liquor content in underflow slurry that flow in one direction. Then the underflow slurry liquor is diluted with wash liquor that flows in the opposite direction and the suspended solids are concentrated again.

The amount of liquor in the thickener underflow contributes to determining the number of CCD stages required to recover the desired amount of soluble metal.

Preliminary testwork was performed on leached ore in order to define approximate size of leached ore in CCD circuit thickeners.

The settling testwork included series of bench scale settling tests to identify correlation between flocculant dose applied and feed slurry dilution with free settling rate which then was used as a Conventional Thickener sizing criteria by Coe and Clevenger method. Another settling test was carried out to define correlation of underflow density with the compaction time (24 h).

Due to the shortage of fresh leached sample, samples of one month and older were re-pulped with liquor and then used for settling test work in order to identify flocculant dose and optimal dilution conditions. Once such conditions are identified and sufficient amount of fresh leached material accumulated confirmation tests should be carried out to ensure “sample ageing” factor is eliminated.

Solids density was defined as 2320 kg/m3, and liquor density used was 1075 kg/m3, which was obtained by dilution of 50 g/l of Mn, 1150 kg/m3 liquor with DI water 1:1. All settling tests were carried out at ambient temperature and pH of the slurry was adjusted to 1.

1L glass cylinders were used to measure solids settling rates after flocculant was applied to the slurry of various densities.

Curves representing settling rates at different flocculant doses and slurry dilutions are shown in Figure 17.

Figure 17:
Settling Rates for Different Flocculant Dose and Pulp Density

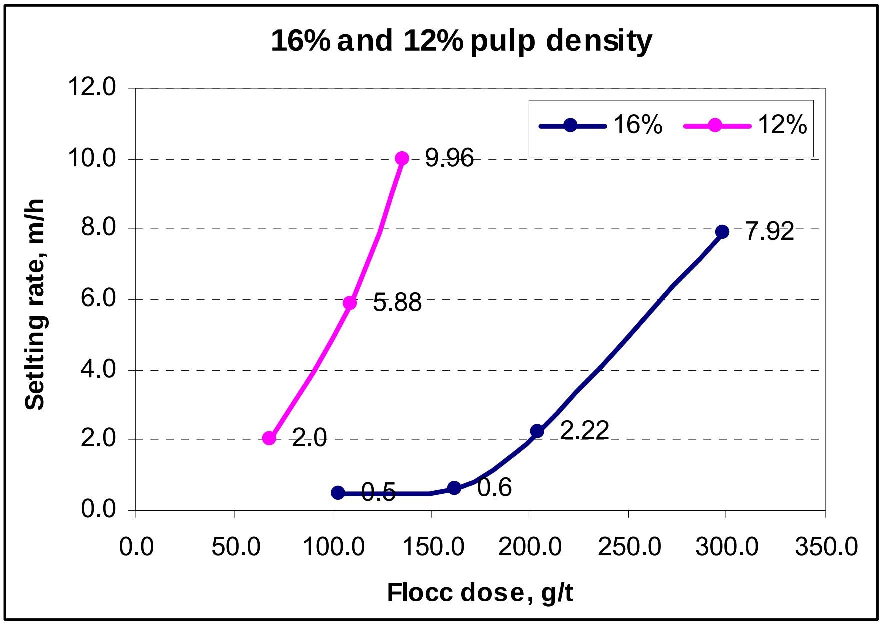

Settling rates of 24% slurry were also measured at various flocculant doses but they are not shown on the graph because they were very low (less then few mm per min) and far out of practical range.

Practically usable settling rates are found at a solids concentration of less than 16 % wt and flocculant application rate of 150-200 gram of E351 (Ciba) per tone of solids. Flocculant dose applied to the slurry seems to be high and flocculant screening series of settling test are needed to identify more efficient type.

Together with settling rates turbidity of supernatant solution was measured and results are given in Figure 18.

Figure 18:
Turbidity of Supernatant

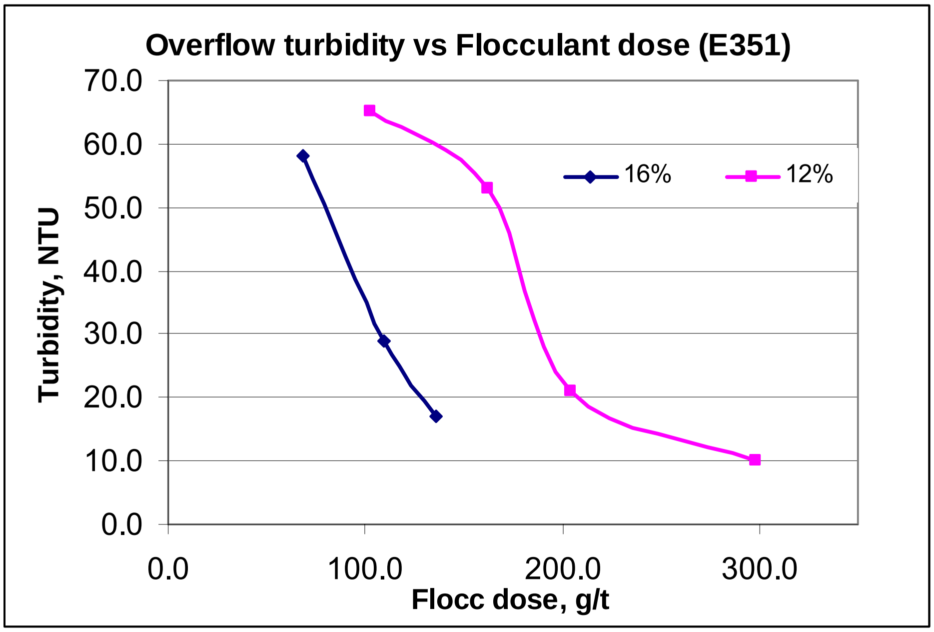

Compaction test for 30% slurry (24 hrs) carried out in 2L cylinder (flocculation rate – 150 g/t) showed that solids density which can be reached within 24 hour settling is about 45% of solids without raking which can slightly increase density of compacted solids, however in the practice conventional thickeners' residence time is normally no longer than 4 hours which corresponds to 38% of solids content in underflow in this particular case. Compaction curve is given on Figure 19.

Figure 19:
24-Hour Compaction Curve with 30% Pulp Density

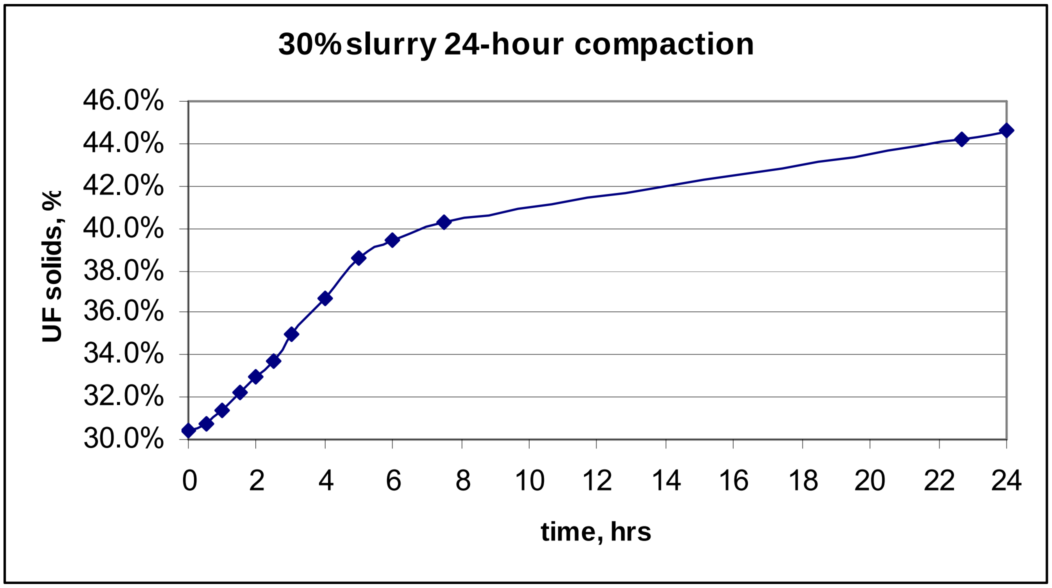

The settling testwork results was used to do preliminary thickeners' sizing of Leached Ore and CCD thickeners

Sizing of Conventional Thickener based on the following criteria:

• Solids loading:	131.3 t/h
• Underflow density:	38% solids w/w
• Feed slurry density:	38-40% of solids w/w
• Dilution (with wash water and/or Auto-dilution):	16%
• Free settling rate:	2.2 m/h

Settling area of the thickener was calculated based on Coe and Clevenger method of conventional thickener sizing and was found to be 216 m2 which corresponds to 17.5 m diameter.

3.4.3 Preliminary Counter Current Decantation Wash Sizing

All calculations were based on preliminary process configuration which comprised of CCD circuit followed by filtration application (dewatering only).

Preliminary evaluated mass balance showed that 5 stage CCD thickener circuit with 2.3 washing ratio (ratio of feed slurry entrained liquid volume to wash liquid volume) washing efficiency sufficient to reach targeted level of overall Mn extraction of 99.5% for 38% solids slurry with 50 g/l Mn content in entrained solution even without taking into account Mn contained in a filtrate recycled from filtration stage.

Figure 20:
CCD Wash Efficiency

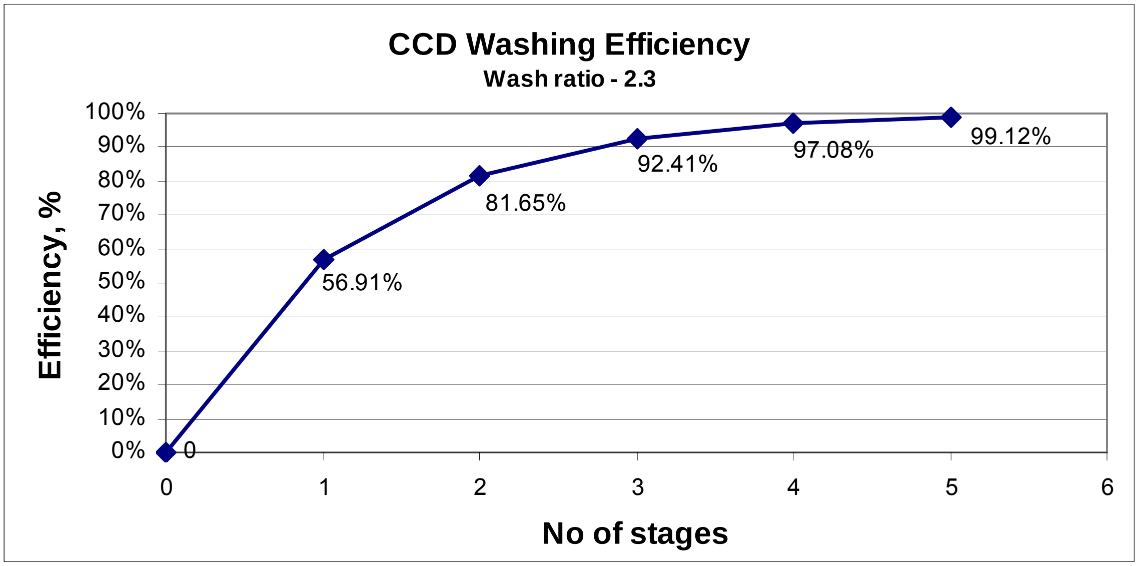

2.3 wash ratio is the maximum feasible that can be reached in case of feed slurry dilution to 16% and corresponds to 0% of thickener overflow recycle (auto-dilution).

Further flowsheet optimization to be done after filtration testwork is carried out and filter cake humidity identified. Lower wash rate would be needed in order to reach the same level of Mn extraction and dilution of feed slurry would be a combination of wash liquid flow and thickener overflow recycling (auto-dilution). For example at filter cake humidity of 15% w/w only 1.6 wash ratio is required for 5-stage CCD circuit or 1.9 for 4-stage CCD.

Suggested process configuration and equipment sizing are not optimized yet and should be revised by equipment manufacturing company based on detailed testwork to be carried out.

As some other options it might be total replacement of CCD circuit by horizontal belt filter application with several washing stages or fewer number of stages CCD circuit followed by vacuum belt filter with one or two washing stages

Use of High Density or Paste thickeners is another option that can give higher solids content in underflow and resulting in less number of CCD stages and/or lower washing ratio, but feasibility of using this type of equipment and questions of handling higher underflow density should be evaluated by solid-liquid separation equipment supplier.

3.4.4 Toxicity Characteristic Leaching Procedure on Tailings

The Toxicity Characteristic Leaching Procedure (TCLP) is EPA Test Method 1311, which is used to simulate leaching through a landfill. This test method is used to determine if a material is classified as a hazardous waste.

TCLP testing was conducted on two solid tailings produced from the testwork on the American Manganese resource. Sample #100608-1 consists of leach residue that was treated with lime to reach a neutral pH. Sample #100608-2 consists of leach residue that was only rinsed and dried before TCLP testing. The results of the TCLP tests are provided in Table 13. The results show that in both cases the American Manganese tailings passed the TCLP tests and are not considered hazardous waste as defined by The Code of Federal Regulations. Table 14 outlines the maximum concentration of contaminants required for non-hazardous classification[15].

Table 13:
TCLP Test Results on American Manganese Leach Residue

TCLP METALS (SOLID)

Maxxam ID		U65605	U65606		
Sampling Date					
COC Number		537548	537548		
	Units	**100608-1**	**100608-2**	**RDL**	**QC Batch**
Metals					
LEACHATE Antimony (Sb)	mg/L	<0.1	<0.1	0.1	4019505
LEACHATE Arsenic (As)	mg/L	0.4	<0.1	0.1	4019505
LEACHATE Barium (Ba)	mg/L	0.2	0.3	0.1	4019505
LEACHATE Beryllium (Be)	mg/L	<0.1	<0.1	0.1	4019505
LEACHATE Boron (B)	mg/L	<0.1	<0.1	0.1	4019505
LEACHATE Cadmium (Cd)	mg/L	<0.1	<0.1	0.1	4019505
LEACHATE Chromium (Cr)	mg/L	<0.1	<0.1	0.1	4019505
LEACHATE Cobalt (Co)	mg/L	<0.1	<0.1	0.1	4019505
LEACHATE Copper (Cu)	mg/L	0.3	<0.1	0.1	4019505
LEACHATE Iron (Fe)	mg/L	<0.5	<0.5	0.5	4019505
LEACHATE Lead (Pb)	mg/L	<0.1	<0.1	0.1	4019505
LEACHATE Mercury (Hg)	mg/L	<0.002	<0.002	0.002	4019505
LEACHATE Molybdenum (Mo)	mg/L	0.4	<0.1	0.1	4019505
LEACHATE Nickel (Ni)	mg/L	<0.1	<0.1	0.1	4019505
LEACHATE Selenium (Se)	mg/L	<0.1	<0.1	0.1	4019505
LEACHATE Silver (Ag)	mg/L	<0.1	<0.1	0.1	4019505
LEACHATE Thallium (Tl)	mg/L	0.9	0.2	0.1	4019505
LEACHATE Uranium (U)	mg/L	<0.1	<0.1	0.1	4019505
LEACHATE Vanadium (V)	mg/L	<0.1	<0.1	0.1	4019505
LEACHATE Zinc (Zn)	mg/L	0.1	<0.1	0.1	4019505
LEACHATE Zirconium (Zr)	mg/L	<0.1	<0.1	0.1	4019505

RDL = Reportable Detection Limit

---

[15] Code of Federal Regulations, http://ecfr.gpoaccess.gov

Table 14:
Maximum Concentration of Contaminants for the Toxicity Characteristic

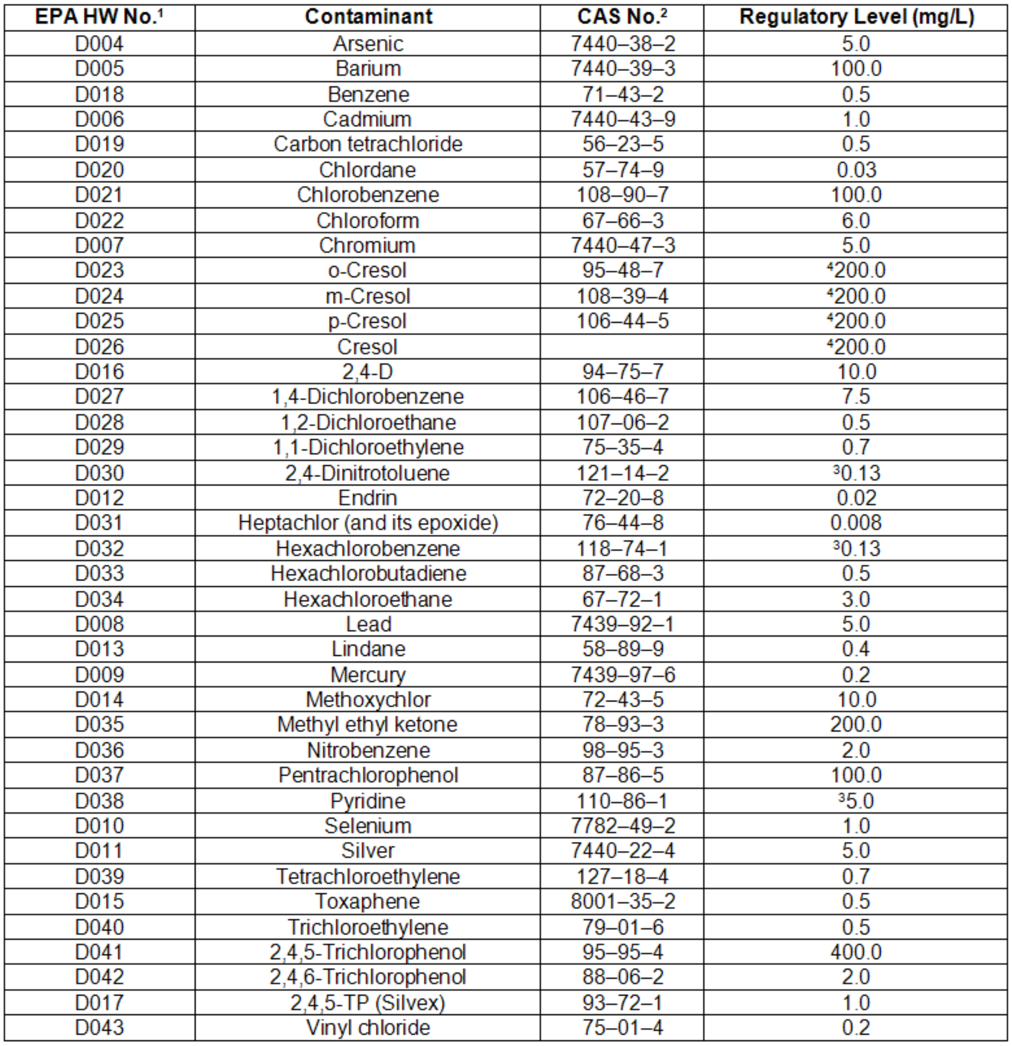

EPA HW No.[1]	Contaminant	CAS No.[2]	Regulatory Level (mg/L)
D004	Arsenic	7440–38–2	5.0
D005	Barium	7440–39–3	100.0
D018	Benzene	71–43–2	0.5
D006	Cadmium	7440–43–9	1.0
D019	Carbon tetrachloride	56–23–5	0.5
D020	Chlordane	57–74–9	0.03
D021	Chlorobenzene	108–90–7	100.0
D022	Chloroform	67–66–3	6.0
D007	Chromium	7440–47–3	5.0
D023	o-Cresol	95–48–7	[4]200.0
D024	m-Cresol	108–39–4	[4]200.0
D025	p-Cresol	106–44–5	[4]200.0
D026	Cresol		[4]200.0
D016	2,4-D	94–75–7	10.0
D027	1,4-Dichlorobenzene	106–46–7	7.5
D028	1,2-Dichloroethane	107–06–2	0.5
D029	1,1-Dichloroethylene	75–35–4	0.7
D030	2,4-Dinitrotoluene	121–14–2	[3]0.13
D012	Endrin	72–20–8	0.02
D031	Heptachlor (and its epoxide)	76–44–8	0.008
D032	Hexachlorobenzene	118–74–1	[3]0.13
D033	Hexachlorobutadiene	87–68–3	0.5
D034	Hexachloroethane	67–72–1	3.0
D008	Lead	7439–92–1	5.0
D013	Lindane	58–89–9	0.4
D009	Mercury	7439–97–6	0.2
D014	Methoxychlor	72–43–5	10.0
D035	Methyl ethyl ketone	78–93–3	200.0
D036	Nitrobenzene	98–95–3	2.0
D037	Pentrachlorophenol	87–86–5	100.0
D038	Pyridine	110–86–1	[3]5.0
D010	Selenium	7782–49–2	1.0
D011	Silver	7440–22–4	5.0
D039	Tetrachloroethylene	127–18–4	0.7
D015	Toxaphene	8001–35–2	0.5
D040	Trichloroethylene	79–01–6	0.5
D041	2,4,5-Trichlorophenol	95–95–4	400.0
D042	2,4,6-Trichlorophenol	88–06–2	2.0
D017	2,4,5-TP (Silvex)	93–72–1	1.0
D043	Vinyl chloride	75–01–4	0.2

3.5 PREGNANT LEACHATE PURIFICATION

As manganese has a high negative value in the electromotive series, the levels of other metals with high reduction potential should be controlled very tightly. As an example, for manganese metal electrodeposition, the impurity content in the solution feed is limited to <0.5 ppm Co, <10 ppm Fe, <1 ppm Ni and <5 ppm Cu, <1000 ppm Al.

As discussed in the manganese extraction section, the main impurities present in the manganese pregnant solution are iron, aluminum, arsenic and silica. Small amounts of zinc, cobalt and copper are also present, their levels depending on the pulp density and the concentration of sulphuric acid used. Typical impurities levels in pregnant solutions obtained at various pulp densities and pH below 1 are given in Table 15.

Increasing the pH to above 5.5, reduced the levels of aluminum, arsenic, iron to below 1 ppm and significantly diminished the silica and copper levels. The pH adjustment had little impact on zinc and cobalt.

Table 15:
Typical impurities in pregnant manganese solutions

	PLS 1	**PLS 2**	**PLS3**
Pulp density during Mn extr	**10%**	**27%**	**40%**
H_2SO_4 conc	**0.05M**	**0.05M**	**0.5M**
Element	**ppm**	**ppm**	**ppm**
Al Aluminium	102	224	689
As Arsenic	42.0	47.3	166
Ca Calcium	1724	1082	558
Cd Cadmium	1.11	<0.1	<0.1
Co Cobalt	1.16	2.84	10.2
Cu Copper	5.55	12.0	21.1
Fe Iron	269	453	1307
K Potassium	249	345	1119
Mg Magnesium	99.7	261	520
Mn Manganese	11413	23443	58467
Mo Molybdenum	<1.	<1.	<1.
Na Sodium	587	1551	2805
Ni Nickel	<0.5	<0.5	<0.5
Pb Lead	<2.	<2.	<2.
Si Silicon	90.2	212	106
Sn Tin	<2.	<2.	<2.
Zn Zinc	31.9	66.4	1511

Removal of copper, zinc and cobalt is usually done by selectively precipitating them as sulphides, as shown in the reaction below. $(NH_4)_2S$, NaHS, Na_2S or even H_2S can all be used as sources of sulphide; in our experiments NaHS was utilized.

$$Zn^{2+} + S^{2-} \rightarrow ZnS \qquad (28)$$

An example of pregnant manganese solution composition before and after purification is given in Table 16. Sulphide precipitation of zinc and cobalt is best done at neutral pH. Excess S^{2-} should be avoided, as residual sulphides could report to the electrolytic manganese metal during the electrolysis.

Table 16:
Manganese purification example

	PLS pH ~ 1	PLS pH ~ 5.6	PLS after NaHS treatment pH ~ 5.6
Al Aluminium	291	6.30	2.52
As Arsenic	35.63	<2.	<2.
Ca Calcium	893	831	880
Cd Cadmium	<0.1	<0.1	<0.1
Co Cobalt	1.98	1.75	<0.5
Cu Copper	9.56	<1.	<1.
Fe Iron	354	1.19	<1.
K Potassium	329	341	334
Mg Magnesium	264	1754	1739
Mn Manganese	17006	16690	16600
Mo Molybdenum	<1.	<1.	<1.
Na Sodium	1303	1321	1396
Ni Nickel	<0.5	<0.5	<0.5
Pb Lead	<2.	<2.	<2.
Si Silicon	146	16.04	13.11
Sn Tin	<2.	<2.	<2.
Zn Zinc	53.19	23.05	<0.5

3.6 MANGANESE CARBONATE PRECIPITATION

Precipitation of the $MnCO_3$ proceeds according to the following reactions:

$$MnSO_4 + Na_2CO_3 \rightarrow MnCO_3 + Na_2SO_4 \quad (29)$$

$$MnS_2O_6 + Na_2CO_3 \rightarrow MnCO_3 + Na_2S_2O_6 \quad (30)$$

Pregnant leach solution used for the $MnCO_3$ precipitation test was prepared by leaching the Artillery Peak resource with SO_2 in a stirred tank reactor, 40% pulp density by weight and 6 hours. The pregnant leach solution was treated to remove impurities by raising the pH to 6 with sodium hydroxide and air sparging to precipitate Al, As and Fe. After filtering the solids, the filtrate was then treated with a stoichiometric amount of NaHS to precipitate Zn, which was then removed by filtration. 20 litres of the pregnant leach solution of approximately 50 g/L was prepared in this manner.

Manganese precipitation was carried out by addition of 150 g/L Na_2CO_3 slurry, at a stoichiometric ratio of 0.8 carbonate to manganese, to the pregnant leach solution in a stirred tank reactor. Precipitation of $MnCO_3$ occurred instantaneously after the addition of Na_2CO_3 to the pregnant leach solution (Figure 21). After complete precipitation (Figure 22), the $MnCO_3$ precipitate was filtered from the solution by vacuum filtration in a Buchner funnel (Figure 23) to collect a wet cake. The wet cake was re-pulped and washed and filtered again to produce a clean wet cake of $MnCO_3$ (Figure 24). The wet cake was dried in a low temperature oven at 30 ^{o}C to produce dry $MnCO_3$ (Figure 25).

Approximately 1.7 kg of dry $MnCO_3$ was collected, which indicates complete utilization of the Na_2CO_3 added.

Figure 21:
Initiation of $MnCO_3$ Precipitation with the Addition of Na_2CO_3

Figure 22:
Complete Precipitation of $MnCO_3$

Figure 23:
Filtration of the $MnCO_3$ Precipitate

Figure 24:
Wet Cake of $MnCO_3$

Figure 25:
Dry Solids of $MnCO_3$

3.7 WATER RECOVERY, ANHYDROUS SODIUM SULPHATE PRODUCTION AND DITHIONATE DESTRUCTION

Most of the water used in the overall process finds its way to the Na_2SO_4 and $Na_2S_2O_6$ containing solution that is produced after precipitation of $MnCO_3$. Water is recovered with very high energy efficiency by cooling this solution to crystallize $Na_2SO_4 \cdot 10H_2O$ and $Na_2S_2O_6 \cdot 2H_2O$. The mother liquor from the cooling crystallizer will have a significantly reduced concentration of Na_2SO_4 and $Na_2S_2O_6$ and as such can be processed through a nanofiltration system to produce clean water, which can be recycled in the overall process, and a concentrate that can be returned to the crystallizer to remove Na_2SO_4 and $Na_2S_2O_6$.

This process is a significantly more energy efficient method of separating water from the salt compared to evaporation, since it avoids the energy intensive latent heat of vaporization. Recovery of water in this manner is made possible because of the unusual solubility characteristics of Na_2SO_4. As shown in Figure 26[16], the solubility of Na_2SO_4 decrease more than ten-fold when decreasing temperature from 32 to 0 ^{o}C, forming a decahydrate. By

---

[16] W.F. Linke, A. Seidell, “Solubilities of Inorganic and Metal Organic Compounds”, 4th ed., Van Nostrand, 1965.

fortuity, as shown in Figure 27, the solubility of $Na_2S_2O_6$ decreases almost three-fold when decreasing temperature from 30 to 0 °C, forming a dihydrate[17].

The majority of water is recovered from the hydrated crystals by heating the crystals to above 32 °C. At this temperature, $Na_2SO_4{\cdot}10H_2O$ dehydrates to form anhydrous Na_2SO_4, H_2O and $Na_2S_2O_6.2H_2O$. After solid-liquid separation, the H_2O can be sent through the nanofiltration system to produce more clean water. In is important to note that aside from the presence of $Na_2S_2O_6$, this is substantially the same method that is used extensively to process Na_2SO_4 in commercial practice.

Figure 26:
Solubility of Sodium Sulphate versus Temperature

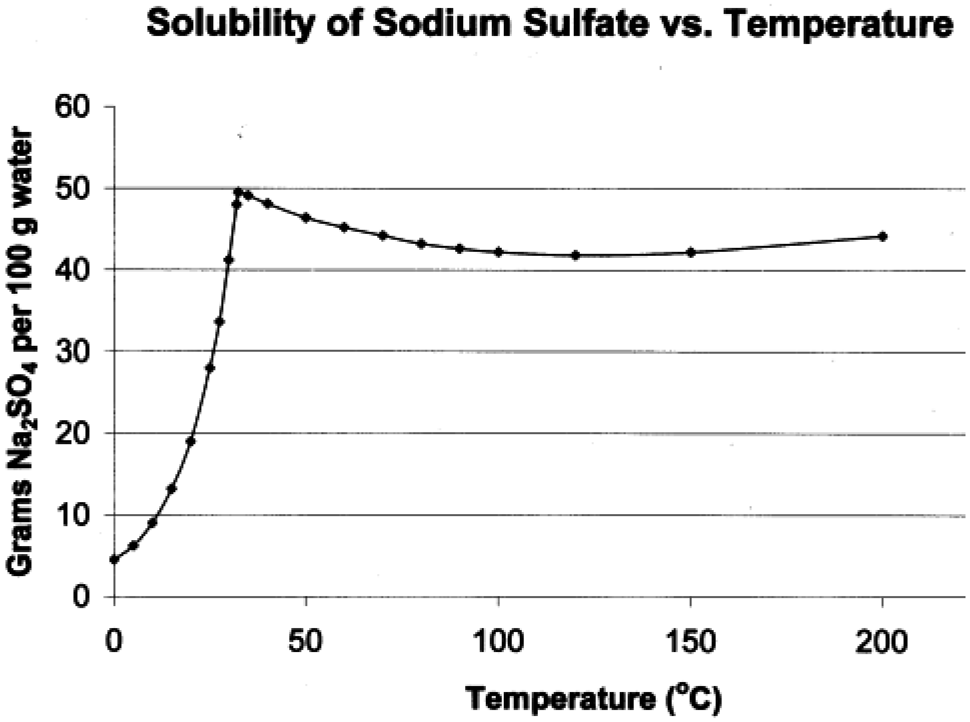

---

[17] W.C. de Baat, "Sur L'Acid Dithionique et Ses Sels", Recueil des Travaux Chimiques des Pays-Bas, vol 45, 1926, pp 237.

Figure 27:
Solubility of Sodium Dithionate versus Temperature

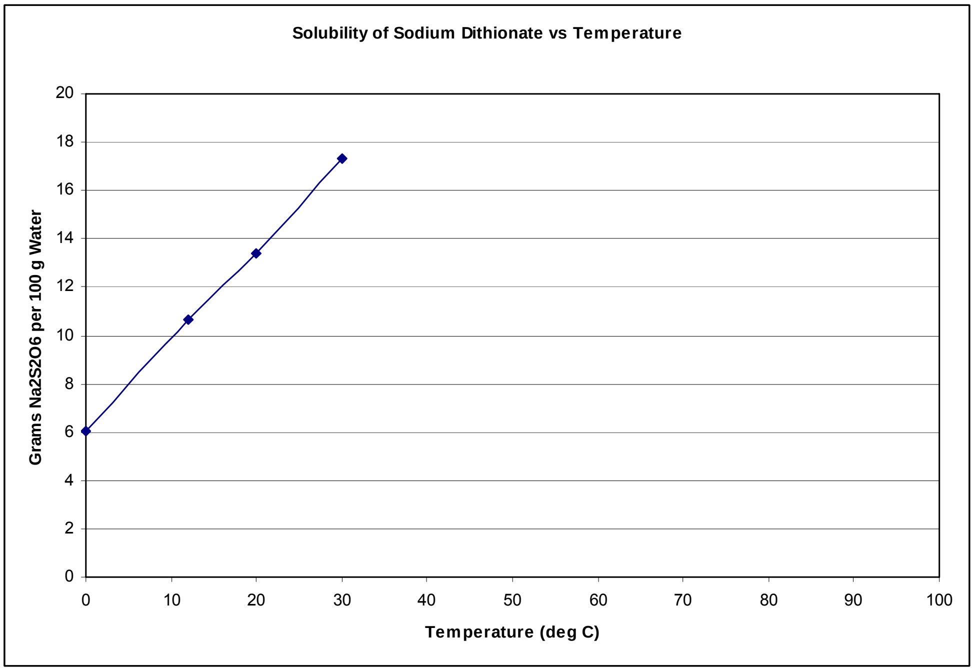

3.7.1 Preliminary Mass Balance

A complete preliminary mass balance was conducted on the process that relates to water recovery, anhydrous sodium sulphate generation and dithionate destruction. This mass balance is provided in Table 17.

Table 17:
Preliminary Mass Balance for Water Recovery, Anhydrous Na_2SO_4 Production and Destruction of Dithionates

Mn Production	
Weight of Ore Processed (Metric Tonnes per day)	3500
Mn Grade (%)	4.50%
Recovery (%)	90%
Mn Production (Metric Tonnes per day)	141.75
Leaching	
Molar Excess SO2 Used in Leach (%)	10%
Concentration of PLS (g Mn per kg solution)	50
Weight of MnSO4 Produced (Metric Tonnes per day)	350.7
Weight of MnS2O6 Produced (Metric Tonnes per day)	55.5
Weight of Water in PLS (Metric Tonnes per day)	2428.9
Manganese Carbonate Precipitation	
Weight of Na2CO3 Required (Metric Tonnes per day)	273.5
Weight of MnCO3 Produced (Metric Tonnes per day)	296.6
Weight of Na2SO4 in By-Product Solution (Metric Tonnes per day)	329.8
Weight of Na2S2O6 in By-Product Solution (Metric Tonnes per day)	53.2
Weight of Water in By-Product Solution (Metric Tonnes per day)	2428.9
Cooling Crystallizer	
Solubility of Na2SO4 at 0 deg C (g/kg water)	11
Solubility of Na2S2O6 at 0 deg C (g/kg water)	60
Weight of Water from Nanofiltration Recycle (Metric Tonnes per day)	1319.8
Weight of Water from Carbonate Precipitation (Metric Tonnes per day)	2428.9
Total Weight of Water Input to Cooler (Metric Tonnes per day)	3748.6
Weight of Na2SO4 Input to Cooler (Metric Tonnes per day)	371.0
Weight of Na2S2O6 Input to Cooler (Metric Tonnes per day)	277.5
Weight of Na2SO4.10H20 Output Crystals (Metric Tonnes per day)	748.2
Weight of Na2S2O6.2H2O Output Crystals (Metric Tonnes per day)	62.5
Weight of Water in Mother Solution (Metric Tonnes per day)	3321.0
Weight of Na2SO4 in Mother Solution (Metric Tonnes per day)	41.1
Weight of Na2S2O6 in Mother Solution (Metric Tonnes per day)	224.4
Dehydration	
Water Recovery from Dehydration of Na2SO4.10H2O (Metric Tonnes per day)	418.3
Nanofiltration	
Weight of Water Input (Metric Tonnes per day)	3739.3
Clean Water Output (Metric Tonnes per day)	2419.6
Weight of Water in Concentrate Recycle (Metric Tonnes per day)	1319.8
Concentration of Na2SO4 Input (g/kg water)	11.0
Concentration of Na2S2O6 Input (g/kg water)	60.0
Concentration of Na2SO4 in Concentrate (g/kg water)	31.2
Concentration of Na2S2O6 in Concentrate (g/kg water)	170.0
Nanofiltration Efficiency	64.7%
Calcination	
Na2SO4 Input (Metric Tonnes per day)	329.8
Na2S2O6.2H2O Input (Metric Tonnes per day)	62.5
SO2 Output (Metric Tonnes per day)	16.5
H2O Output (Metric Tonnes per day)	9.3
Na2SO4 Output (Metric Tonnes per day)	366.5
Water Recovery	
% Water Recovery of Process	100.0%

3.7.2 Calculated Preliminary Energy Balance

In order to conduct a preliminary energy balance for water recovery, anhydrous sodium sulphate production and destruction of dithionates to recover SO_2, the data summarized in Table 18 is required.

Table 18:
Thermodynamic Data Required for Energy Balance Calculations

THERMODYNAMIC DATA	REFERENCE
Latent Heat of Vaporization (H_2O) = 2260 KJ/kg	12
C_p (H_2O $_{liquid}$) = 4.186 (KJ/kg ^oC)	12
C_p ($Na_2SO_4{\cdot}10H_2O$) = 499.3 (J/mol ^oC)	12
C_p (Na_2SO_4) = 128.2 (J/mol ^oC)	12
C_p ($Na_2S_2O_6{\cdot}2H_2O$) = Data Not Available, Estimate as $Na_2SO_4{\cdot}10H_2O$	
ΔH ($Na_2SO_4{\cdot}10H_2O$) = -4327.26 (KJ/mol)	12
ΔH (Na_2SO_4) = -1387.1 (KJ/mol)	12
ΔH (H_2O $_{liquid}$) = -285.83 (KJ/mol)	12
ΔH ($Na_2S_2O_6{\cdot}2H_2O$) = Data Not Available, Estimate as ΔH ($MnS_2O_6{\cdot}2H_2O$)	
ΔH ($MnS_2O_6{\cdot}2H_2O$) = -1991.2 (KJ/mol)	18
ΔH ($MnSO_4$) = -1065.3 (KJ/mol)	12
ΔH (SO_2) = -296.81 (KJ/mol)	12
ΔH (H_2O $_{gas}$) = -241.86 (KJ/mol)	12

The energy requirements to operate reverse osmosis for desalination was estimated at 2 KWh per m^3 of water processed[19] (used to estimate energy consumption for nanofiltration).

According to Tammann[20] et al $Na_2S_2O_6{\cdot}2H_2O$ decomposes at 267 ^oC, evolving SO_2 gas.

---

[18] Feng Guozhong Lei Yidong, “The Measurements of Thermodynamic Functions of Manganese Dithionate Hydrates”, Journal of Guangxi University (Natural Science Edition), Vol. 2, 1992

[19] P. Geisler, W. Krumm , and T.A. Peters, “Reduction of the energy demand for seawater RO with the pressure exchange system PES”, Desalination, Vol. 135, 2001, pp. 205-210.

Using a design basis of 141.75 metric tonnes per day of Mn production and a pregnant leachate concentration of 50 g Mn per kg water, the following energy balance was calculated by Kemetco (Table 19).

Table 19:
Calculated Preliminary Power Requirements to Recover Water, Process Anhydrous Sodium Sulphate and Decompose Dithionates

American Manganese Water Recovery and Dithionate Destruction Process	**MW**
Power to Chill Na_2SO_4 + $Na_2S_2O_6$ Solution from 25 °C to 0 °C and Crystallize $Na_2SO_4 \cdot H_2O$ and $Na_2S_2O_6 \cdot 2H_2O$	7.77
Power to Heat Crystals from 0 °C to 40 °C	0.60
Power for Nanofiltration	0.25
Power to Calcine Na_2SO_4 and $Na_2S_2O_6 \cdot 2H_2O$ Crystals to 267 °C	1.55
Heat Recovery from Mother Liquid at 0 °C	-4.34
Low Grade Heat Recovery from Sulphur Burner Exhaust for Calcine	-0.81
Low Grade Heat Recovery from Sulphur Burner Exhaust for Heating Crystals	-0.60
Total Power with American Manganese Process	**4.42**

3.7.3 Preliminary Energy Balance Using Data Provided by a Commercial Supplier of Sodium Sulphate Production Plants

Swenson Technology Inc is a commercial supplier of sodium sulphate crystallizer systems. Swenson was provided operating conditions for treatment of the Na_2SO_4 and $Na_2S_2O_6$ solution stream in the American Manganese process. Based on this information, Swenson provided a preliminary flowsheet, shown in Figure 28, with preliminary process power requirements.

Using the data provided by Swenson's flowsheet, process power requirements were calculated and summarized in Table 20.

---

[20] Von G. Tammann, W. Boehme, "Zur Zersetzung der Dithionate", Zeitschrift Für Anorganische und Allgemeine Chemie, Vol. 204, 1932, pp 144.

Table 20:
Calculated Preliminary Energy Balance to Recover Water, Process Anhydrous Sodium Sulphate and Decompose Dithionates Using Data from Swenson

American Manganese Water Recovery and Dithionate Destruction Process	**HP**	**mmBTU/hr**	**MW**
Power to Chill Na_2SO_4 + $Na_2S_2O_6$ Solution from 25 °C to 0 °C and Crystallize $Na_2SO_4 \cdot H_2O$ and $Na_2S_2O_6 \cdot 2H_2O$	1500		1.10
Power to Heat Crystals from 0 °C to 40 °C		7.5	2.20
Power for Nanofiltration	1200		0.88
Power to Calcine Na_2SO_4 and $Na_2S_2O_6 \cdot 2H_2O$ Crystals to 267 °C (Not Provided by Swenson, used data in Table 19)			1.55
Low Grade Heat Recovery from Sulphur Burner Exhaust for Calcine (Not Provided by Swenson, used data in Table 19)			-0.81
Low Grade Heat Recovery from Sulphur Burner Exhaust for Heating Crystals (Not Provided by Swenson, used data in Table 19)			-1.30
Total Power with American Manganese Process			**3.62**

Figure 28:

Preliminary Flowsheet for Recovery of Water, Production of Anhydrous Sodium Sulphate, and Destruction of Dithionates (data from Swenson Technology Inc.)

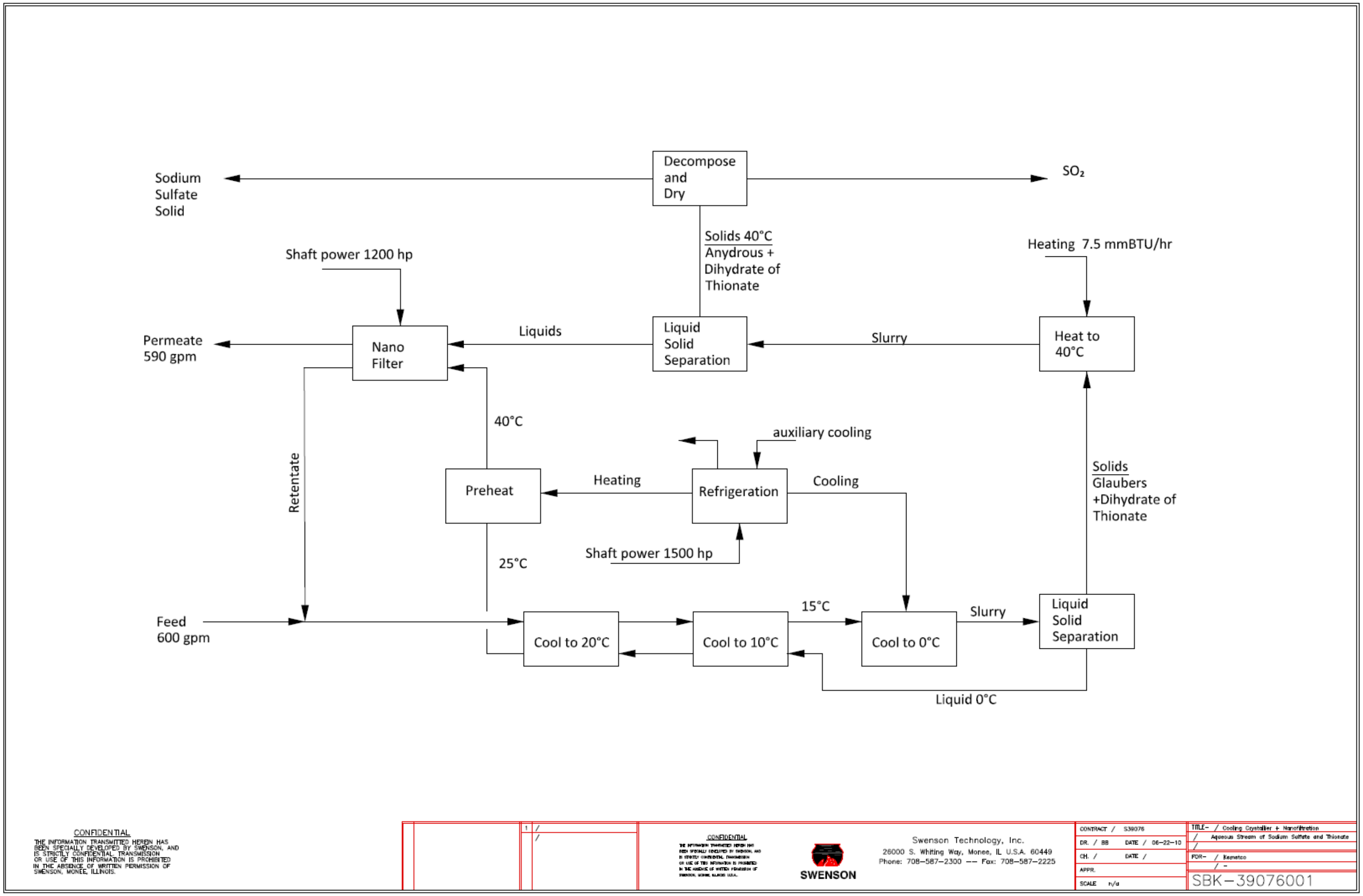

3.7.4 Comparing Energy Balance with Data from a Commercial Sodium Sulphate Plant

In order to compare the calculated energy balance to recover water, produce anhydrous sodium sulphate and decompose dithionates, detailed operating data for a commercial sodium sulphate production plant was obtained. The commercial sodium sulphate production plant is operated by Laguna del Rey, in Mexico and a flowsheet of the operation is provided in Figure 29[21].

Figure 29:
Flowsheet for the Laguna del Rey Sodium Sulphate Plant

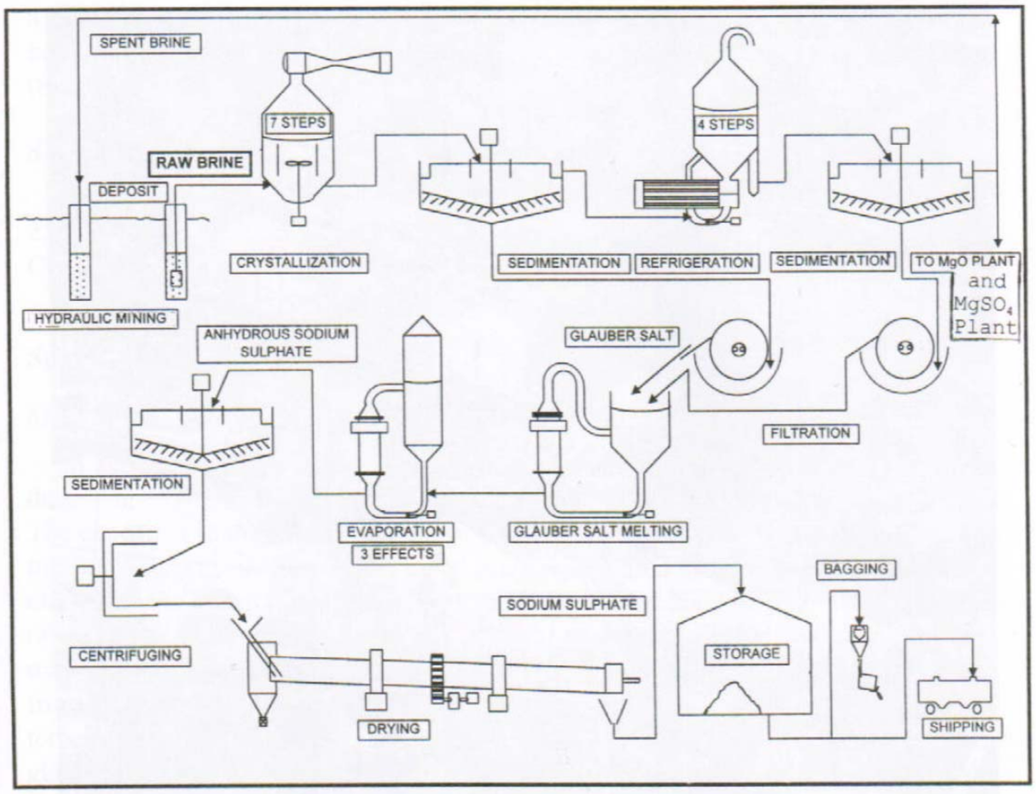

Figure 4.15 Flow sheet for the Laguna del Rey sodium sulfate plant. (From Ross, 1999, courtesy of Servicios Industrias Penoles, S.A. de C.V.)

Operating data for the Laguna del Rey sodium sulphate plant is summarized and compared to the calculated operating conditions of the American Manganese plant (see Table 21). Similarities between the calculated installed power per unit production of Na_2SO_4 supports the technical and economical viability of this approach for the American Manganese process.

---

[21] Donald E. Garrett, “Sodium Sulfate, Handbook of Deposits, Processing, Properties, and Use”, Academic Press, 2001, pp 220 – 225.

Table 21:
Comparison of Operating Conditions between the Laguna del Rey Sodium Sulphate Plant and the Proposed American Manganese Plant.

	Laguna del Rey, Mexico[21] (Operating)	American Manganese Inc (Proposed)
Anhydrous Na_2SO_4 Production Metric Tonnes Per Year	620,000	133,773
Concentration of Na_2SO_4 (g/L)	200	150
Volume Flow Rate (L/min)	6800	1687
Installed Power (MW)	14	3.62 - 4.42
Calculated Energy Consumption (KWh/Tonne Na_2SO_4)	198	237 - 290

3.7.5 Comparing Energy Balance with Simple Evaporation

In order to show the dramatic difference in process power required to recover water using the American Manganese process versus simple evaporation, an energy balance between both approaches are summarized in Table 22. The calculations are based on 141.75 metric tonnes per day Mn production and a pregnant leachate concentration of 50 g/L.

Table 22:
Comparison of Power Usage to Recover Water by Simple Evaporation versus the American Manganese Process.

Power Requirements for Simple Evaporation	**MW**
Specific Heat to Raise Temperature From 25 °C to 100 °C	8.83
Latent Heat Requirements for Simple Evaporation	63.53
Low Grade Heat Recovery from Sulphur Burner Exhaust to 100 °C	-1.79
Total Power with Simple Evaporation	**70.57**
American Manganese Water Recovery and Dithionate Destruction Process	**MW**
Power to Chill Na_2SO_4 + $Na_2S_2O_6$ Solution from 25 °C to 0 °C and Crystallize $Na_2SO_4 \cdot 10H_2O$ and $Na_2S_2O_6 \cdot 2H_2O$	7.77
Power to Heat Crystals from 0 °C to 40 °C	0.60
Power for Nanofiltration	0.25
Power to Calcine Na_2SO_4 and $Na_2S_2O_6 \cdot 2H_2O$ Crystals to 267 °C	1.55
Heat Recovery from Mother Liquid at 0 °C	-4.34
Low Grade Heat Recovery from Sulphur Burner Exhaust for Calcine	-0.81
Low Grade Heat Recovery from Sulphur Burner Exhaust for Heating Crystals	-0.60
Total Power with American Manganese Process	**4.42**

Table 22 shows that the energy required to recover water from the process stream containing Na_2SO_4 and $Na_2S_2O_6$ in the American Manganese conceptual process is approximately 6% of that required if done so by conventional evaporation techniques. The latent heat of vaporization accounts for the majority of the power requirement for evaporation. The use of mechanical vapour recompression (MVR) evaporation technology can recover some of the latent heat by recompressing the vapour phase so that heat can be recovered by heat exchange. MVR evaporation can also significantly reduce power consumption in evaporation since a significant amount of the latent loss can be recovered. Prior to considering MVR evaporation, extensive corrosion studies should be conducted, since MVR units are expensive equipment. Evolution of SO_2 gas mixed with water would create a corrosive environment within the MVR components.

3.7.6 Dithionate Thermal Decomposition Testwork

In order to better investigate the conditions required to effectively destroy dithionates using MnO_2 and isolate other interferences, a scoping test using reagent grade chemicals was performed. For this test, a solution containing 20g/L sodium dithionate was contacted with excess MnO_2 for 24 hours. The dithionate concentration remained constant when no sulphuric acid was added, but dropped to 18.7g/L and 17.2 g/L in the presence of 0.8M and 1.6M H_2SO_4, respectively. This suggests that dithionates can be decreased by excess MnO_2 and acid, although the high requirement of sulphuric acid makes the approach less attractive from an economic point of view.

Thermal decomposition proved to be a successful strategy to eliminate the dithionates. The first thermal decomposition test was performed on a pregnant solution produced during a bottle test. In a first stage, the water was evaporated at around 105^{o}, producing a salt containing about 5.6% dithionates. The resulting salt was then placed in an oven and the temperature was slowly increased and maintained at $400^{o}C$ for 30 minutes. Salt samples were removed at $200^{o}C$ and $400^{o}C$ and the dithionates were analyzed by ion chromatography. The dithionates analysis revealed that more than 80% dithionates were removed at $200^{o}C$, while complete decomposition was achieved at $400^{o}C$.

The goal of the second test was to determine the lowest temperature required for complete dithionate decomposition. 50 mL pregnant solution from a bottle roll test containing approximately 48g/L dithionates was placed overnight in an oven, at $75^{o}C$, to evaporate the water. The resulting salt, containing 10.2% dithionates, was then slowly heated to $400^{o}C$ in $50^{o}C$ increments. Solid samples were removed at 150, 200, 250, 300 and $400^{o}C$ and the dithionates were analyzed by IC. Surprisingly, complete destruction of dithionates was observed at $250^{o}C$, a much lower temperature than previously reported by Hazen Research (1977). In fact, the dithionate content was reduced by approx 80% by drying alone. The thermal decomposition approach has the advantage of allowing the recovery and recirculation of sulphur dioxide that otherwise would be lost.

3.7.7 Use of a Bioreactor to Reduce Dithionates

An alternative process scheme that uses a proprietary bioreactor to destroy dithionates, and recover SO_2, energy and sodium bicarbonate ($NaHCO_3$) was tested. While mass and energy balances have not been conducted during this preliminary work, testing of the bioreactor has shown that biological reduction of $Na_2S_2O_6$ can be achieved at a significantly higher rate than biological reduction of Na_2SO_4.

As a proof of concept, a gas-fed continuous laboratory reactor was set-up (Figure 30) and operated. Sulphite reducing bacteria population was transferred from an existing bio-reactor developed by Kemetco and a 15g/L dithionate solution with trace micro-nutrients (KH_2PO_4, $MgSO_4$, $(NH_4)_2SO_4$, $CaCl_2$, NaCl and $FeSO_4$) was pumped through as a feed solution. Gaseous feed such as CO, CO_2 and H_2 were also added. The net reaction in the bioreactor is as follows:

$$Na_2S_2O_6 + 2CO + 5H_2 \rightarrow 2H_2S + 2NaHCO_3 + 2H_2O \qquad (31)$$

In concept, the H_2S generated by the bioreactor can be burned to produce energy and recover SO_2 to be recycled back to the leach. The $NaHCO_3$ bioreactor product can be used to precipitate Mn for recovery from the pregnant leach solution.

Figure 30:
Gas Fed Bioreactor

Biological dithionate reduction testing was initiated with the filling of a 1.4 litre up-flow gas-fed bioreactor using a combination of synthetic sodium dithionate solution and discharge solution from another bioreactor operating on a sulphite feed solution and using the same gaseous nutrients. A bioreactor schematic diagram is presented in Figure 31.

The reactor was fed semi-continuously at an increasing rate using a sodium dithionate solution containing 15 g/L dithionate along with trace nutrients. The reactor is continuously fed a gas stream containing carbon monoxide, hydrogen and carbon dioxide, simulating the off-gas from a partial oxidation burner. This provides the carbon and energy source for the bacteria as they reduce the dithionate to sulphide and product sodium bicarbonate as a by-product.

The system has been fed at a slow, but increasing, rate for first few weeks to establish the biomass and adapted it to dithionate. Testing has included looking at the effect of varying the gas mix, and the feed solution has been modified to include sulphate at levels that reflect the expected process stream composition. Initial results have been positive, as dithionate reduction has been established relatively quickly. A population capable of continuous dithionate reduction using gaseous nutrients has been established, and the rate of biological activity has increased steadily. The feed was modified to simulate a process feed solution and testing has shown a relative preference to dithionate over sulphate. Gas nutrient testing has shown that the system can operated with carbon monoxide as the principal energy source, but higher rates will likely require hydrogen in the mix. After about 2 ½ months of operation a maximum reduction of 4.095 g/L/day of dithionate as equivalent sulphate was reached.

Figure 31:
Bioreactor Set-up

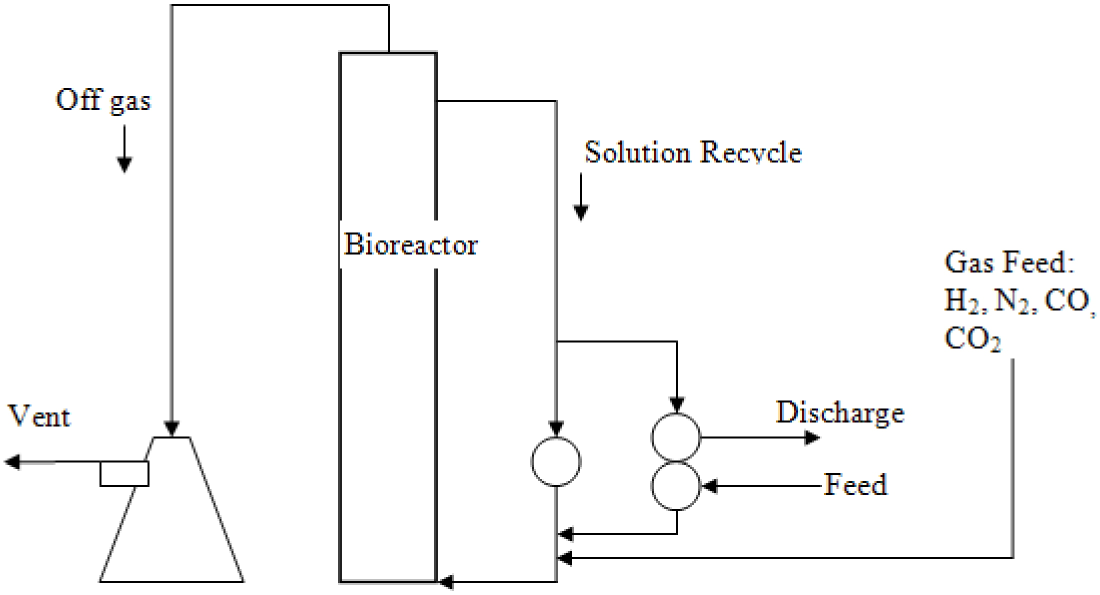

The work so far has demonstrated that there is no biological barrier to using dithionate as the sulphur source for reducing bacteria. Population adaptation has proceeded smoothly. To evaluate the economic potential, however, the system will need to be operated at much higher levels to determine the unit reduction rates that are possible. This in turn will provide guidance in sizing bioreactors that would be required on a commercial scale.

3.7.8 Autoclave Testing

As part of the dithionate destruction testwork, a high pressure autoclave was purchased and set up for conducting high pressure and temperature oxidation tests on pregnant leach solution containing MnS_2O_6. A photograph of the autoclave setup is show in Figure 32.

500 mL pregnant solution containing approx 57g/L Mn, 40 g/L dithionate and other impurities such as Ca (200 ppm), Al (573 ppm), Fe (1179 ppm), Zn (153 ppm) was placed in the 1L reactor. The solution was heated to about 200°C, while the pressure reached 280 psi. Once the desired temperature and pressure were achieved, O_2 was fed into the reactor to attain a total pressure around 390 psi (110 psi O_2 over pressure). The oxygen feed was then cut off, in an effort to monitor the O_2 consumption during the reaction. The O_2 over

pressure dropped from 110 psi to about 60 psi in the first 15 minutes, after which O_2 was added to bring the total pressure back to 390 psi. No significant oxygen consumption was observed afterwards. Samples were collected at 30, 60 and 90 minutes. The sample collected at 90 minutes was cloudy and exhibited a strong greenish color that was later identified as being due to corrosion.

The analysis of the samples collected during the high pressure oxidation test revealed that dithionates were completely oxidized in the first 30 minutes. However, the manganese concentration dropped significantly, from 57g/L to about 20g/L after 1.5 hours. This suggests that Mn^{2+} was likely oxidized to Mn^{4+}. Mn^{3+} and Mn^{4+} compounds are insoluble in sulphuric acid solution and precipitated at the bottom of the autoclave as shown in Figure 33. Another issue that became apparent during the test was the corrosion of the 316 stainless steel, due to the considerable amount of sulphuric acid produced during the pressure oxidation.

Figure 32:
Autoclave set up for high temperature and pressure oxidation

Figure 33:
Precipitate obtained during the autoclave testing

Further autoclave testing was suspended in favour of thermal decomposition of sodium dithionate, which appears to be a simpler approach to dealing with dithionates.

3.8 ELECTROWINNING

3.8.1 Electrolytic Manganese Metal Production Testwork

A divided electrowinning cell (1L solution volume) was designed and constructed to test electrolytic manganese metal production. An isometric design drawing and photograph of the electrowinning cell are shown in Figures 34 and 35 respectively.

Figure 34:
Manganese electrowinning cell

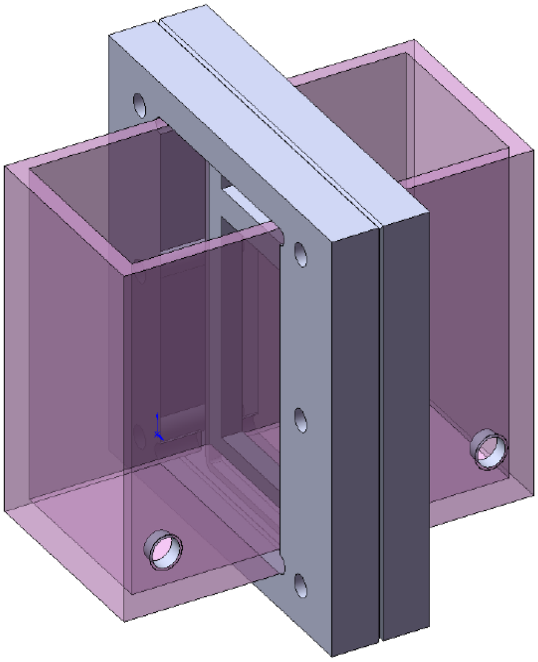

Figure 35:
Photo of Electrowinning cell for electrolytic manganese metal

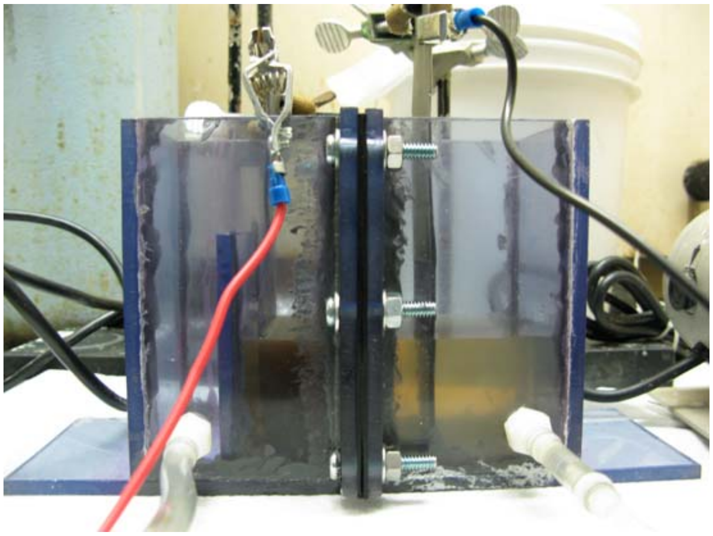

Manganese metal electrowinning tests were conducted in the divided cell. The cell was fitted with a stainless steel 316 cathode of 2 mm thickness and a lead-silver alloy (1% Ag) anode procured from Teck Resources of Trail, BC, Canada. As an initial test, feed manganese sulphate solution was prepared using ACS grades manganese sulphate from Alfa Aesar, ammonium sulphate from Sigma Aldrich and sodium sulphite from Anachemia. The addition of ammonium sulphate to the manganese electrolyte is meant to act as a buffer between pH 3 and 9, preventing the manganese hydroxide precipitation during electrodeposition. In addition, the ammonium sulphate improves the conductivity of the solution. Controlled levels of selenium or reduced sulphur compounds are usually added to increase the current efficiency and reduce the effect of impurities. Although selenium compounds are known to improve the current efficiency, they are a major waste management problem due to high toxicity. As an alternative to selenium, sulphur dioxide was added to the electrowinning cells to improve current efficiency.

The feed solution for the electrowinning tests contained approx 30g/L Mn (as $MnSO_4$), 130 g/L $(NH_4)_2SO_4$ and 1g/L Na_2SO_3. The feed solution was pumped into the cathode chamber at a flow rate of 2 ml/min. The depleted catholyte overflowed into the anode chamber and the anolyte was collected into a spent electrolyte tank. The pH of the feed solution was adjusted to around 6.2 by using either NH_4OH or H_2SO_4. The pH of the catholyte stabilized at pH around 8, while the anolyte pH dropped below 1. A summary of the conditions used in the electrodeposition experiments and the results is given in Table 23.

Table 23:
Electrowinning test conditions and results

Feed	
Mn	30 g/L
$(NH_4)_2SO_4$	130 g/L
Na_2SO_3	1 g/L
pH	6.2
Catholyte	
Mn	15-18 g/L
pH	7.6-8
Flow rate	2 mL/min
Cathode area	66 cm2
Current	2.4
Cathode Current density	360 A/m^2
Temperature	35^oC
Electrodeposition time	18-24 h
Current efficiency	54-55%

A series of manganese electrowinning tests have been carried out, using various operating conditions, in order to determine the parameters that influence the current efficiency. Some of the factors tested so far include Mn, $(NH_4)_2SO_4$, Na_2SO_3 concentrations and the cathodic current density. All tests were performed in an electrolytic cell fitted with a 316 stainless steel cathode, lead or lead-silver (0.5 wt% Ag) alloy anode, using a feed flow rate of 2ml/min.

Electrolyte for the electrowinning tests was prepared with a two stage leach of the resource material. Each stage of leach was conducted in a stirred tank with 40% pulp density, a solution containing 0.5M H_2SO_4 and sparging the slurry with 16% by volume SO_2 mixed with N_2.

More than 90% Mn extraction was achieved after about 7 hours. The concentration of the pregnant leach solution was approximately 50 g/L Mn. The solution also contained 1.3 g/L Fe, 0.7 g/L Al, 140 ppm As, 145 ppm Zn and about 66g/L dithionates. This pregnant solution was used in a subsequent manganese extraction test, to leach a fresh ore sample, with the ultimate goal of obtaining a pregnant solution containing approx 100g/L Mn. Solid-liquid separation was conducted with vacuum filtration.

The final leach solution was characterized by a pH below 1, specific gravity of 1.22 and Mn concentration of 103g/L. This leach solution was placed in an oven at 80 ^oC for 8 hours to evaporate the liquids and crystallize the Mn as $MnSO_4$ crystals. The evaporation was considered completed when approx 60% of the total weight was removed. A small sample of the dry crystals were taken for a dithionate analysis, while the rest was calcined at 250^oC for half hour. The calcined material was cooled, weighed and a small sample was collected for dithionate analysis. The dithionate analysis revealed that more than 85% of the dithionate were removed during the drying at 80^oC, and complete decomposition was achieved after calcining at 250 ^oC for 30 minutes.

The calcined $MnSO_4$ product was later dissolved in DI water, generating a solution with pH around 1. The solution was purified in two stages. In the first stage, $(NH_4)OH$ was added to the solution to bring the pH up to 7, while simultaneously sparging O_2 into the solution. The purpose of the O_2 sparging was to oxidize the ferrous iron to the ferric form. At neutral pH, the ferric iron along with aluminum and arsenic precipitate as hydroxides. The pH adjustment was followed by sulphide precipitation with NaHS. Analyses of the $MnSO_4$ at different stages of production is shown in Table 24.

Table 24:
Solution and crystals analysis subsequent to various unit operations

Element	**Stage #1 Leach**	**Stage # 2 Leach**	**MnSO4 80C**	**MnSO4 250C**	**Mn soln pH >6**	**Mn Soln after S^{2-} ppt**
	mg/L	mg/L	mg/kg	mg/kg	mg/L	mg/L
Ag Silver	<0.5	<0.5	<2.5	<2.5	<0.5	<0.5
Al Aluminium	701	1152	6371	4491	<2.	<2.
As Arsenic	140	272	1595	981	<2.	<2.
B Boron	15.32	33.87	87.4	64.9	7.12	6.89
Ba Barium	<0.1	<0.1	1.51	1.79	0.28	0.24
Be Beryllium	<0.1	<0.1	<0.5	<0.5	<0.1	<0.1
Bi Bismuth	<5.	<5.	<25.	<25.	<5.	<5.
Ca Calcium	587	294	983	1170	231	347
Cd Cadmium	<0.1	<0.1	<0.5	<0.5	<0.1	<0.1
Co Cobalt	4.84	9.96	39.7	32.7	6.36	3.52
Cr Chromium	<0.5	<0.5	13.81	<2.5	<0.5	<0.5
Cu Copper	19.70	42.88	174	128	<1.	<1.
Fe Iron	1392	2456	7428	7600	971	<2
K Potassium	1194	2052	9923	6533	1167	1761
Li Lithium	6.04	11.12	73.8	54.0	9.29	15.59
Mg Magnesium	485	891	4928	3699	669	944
Mn Manganese	49611	103188	253072	295978	99817	102464
Mo Molybdenum	<1.	<1.	<5.	<5.	<1.	<1.
Na Sodium	2404	5185	12948	16096	3021	4867
Ni Nickel	<0.5	<0.5	13.8	12.8	2.35	<0.5
Pb Lead	<2.	<2.	1214	969	<3.	<2.
S Sulfur	61771	95713	195828	209869	46079	71462
Sb Antimony	<2.	<2.	<10.	<10.	<2.	<2.
Se Selenium	10.09	22.13	<25.	<25.	<2.	<2
Si Silicon	79.33	61.45	48.67	32.83	<5.	<5.
Sn Tin	<2.	<2.	<10.	<10.	<2.	<2.
Sr Strontium	7.13	3.59	18.4	17.6	3.29	4.89
Zn Zinc	145	280	1225	972	163	<0.5
Dithionates g/L or g/Kg	60	105	35	-		

Table 24 shows the final Mn^{2+} solution (after sulphide precipitation) to be essentially free of heavy metal contamination.

The initial tests, shown in Table 25, revealed that slightly elevated manganese concentration is one of the key factors influencing the current efficiency. An increase of 10g/L (from 30 to 40g/L) increased the current efficiency to more than 60% (67% when using 150g/L $(NH_4)_2SO_4$). Another parameter impacting the current efficiency is the current density. As expected, a higher current leads to additional H_2 generation at the cathode, lowering the current efficiency. The effect of $(NH_4)_2SO_4$ and Na_2SO_3 (or SO_2) has not been entirely clarified and supplementary work should be conducted to better understand these influences.

Table 25:
Manganese electro deposition conditions and corresponding current efficiencies

Test	Feed Mn conc	$(NH_4)_2SO_4$ conc	Na_2SO_3 conc	Current density	Flow rate	Anode type	Current efficiency
	(g/L)	(g/L)	(g/L)	A/m2	mL/min		(%)
#1	30	130	1	350	2	Pb	55.40%
#2	30	130	1	600	2	Pb	49.80%
#3	30	150	1	350	2	Ag-Pb	52.10%
#4	30	150	2	350	2	Ag-Pb	64.80%
#5	40	130	1	350	2	Ag-Pb	59.60%
#6	40	150	1	350	2	Ag-Pb	67.60%
#7	30	130	2	350	2	Ag-Pb	55.30%

A photograph of sheets of electrolytic manganese metal of > 99.5% purity, electrowon from purified solution is shown in Figure 36.

Figure 36:
Photo of Electrolytic Manganese Metal Electrowon from Purified Leach Solution.

3.8.2 Magnetized Electrodes

A brief study was conducted to examine the effects of magneto-hydrodynamics in reducing cell voltage of a Mn electrowinning cell. Magnetized electrodes were supplied by Prof. Robert O'Brien of MHD Technologies in Victoria, BC. A comparison of the cell voltage for manganese electrowinning was conducted with magnetized electrodes, versus non-magnetized electrodes.

From a brief test, an average voltage reduction of 1.66% was observed with the magnetized electrodes versus the non-magnetized electrodes. Unfortunately, it was determined that the electrodes were plain carbon steel instead of nickel as originally specified. As such, significant corrosion of the electrodes occurred during the electrowinning experiments and further tests were put on hold until new electrodes of the correct material could be procured. This remains to be tested in future work.

3.8.3 Electrolytic Manganese Dioxide Production Testwork

Although the main product is to produce electrolytic manganese metal (EMM), electrolytic manganese dioxide (EMD) is also considered either as an alternative product or as a by-product of the EMM generation.

Electrolytic cells for EMD production consist of open-top tanks fitted with titanium anodes and graphite or metallic cathodes. Unlike for EMM, EMD cells do not require separators.

The electrolysis of $MnSO_4$ to produce MnO_2 can be summarized as follows:

Anode: $Mn^{2+} + 2H_2O \rightarrow MnO_2 + 4H^+ + 2e^-$ (32)

Cathode: $2H^+ + 2e^- \rightarrow H_2$ (33)

Overall: $Mn^{2+} + 2H_2O \rightarrow MnO_2 + 2H^+ + H_2$ (34)

High quality EMD is usually produced at low anode current densities (60-80 A/m^2), but the addition of small EMD particles in the electrolyte allows the production of good quality EMD even at anode densities of 100-200 A/m^2. Temperature, current density and sulphuric acid concentration have a particularly significant effect on the quality of the EMD deposit. Typical conditions used for the EMD productions are given in Table 26.

A scoping manganese dioxide electrodeposition test was performed using the purified leachate produced for earlier EMM electrowinning tests. The test was performed in a beaker fitted with a titanium anode and a graphite cathode, at a temperature of 95^{o}C. Good mixing of the electrolyte was achieved with a magnetic stirrer. The feed solution contained about 150 g/L Mn and the current density was set at 75A/m^2. Fresh feed solution was continuously added to the electrolyte to compensate for the evaporated liquid. After about 5 hours the EMD was harvested and weighed. Based on the deposit weight, a current efficiency of 93% was calculated. A photograph of the product is shown in Figure 37.

Figure 37:
Electrolytic Manganese Dioxide Produced by Electrowinning

Table 26:
Typical conditions for EMD production

Parameter	Typical conditions
$MnSO_4$ feed solution (g/L)	130-160
Anode	Ti
Cathode	Graphite
Temperature (^oC)	95^-98
Cell voltage (V)	2.7- 3
Current density (A/m^2)	60-80

3.9 ENERGY SAVINGS BY AVOIDING ROASTING

In order to illustrate the potential savings of the American Manganese hydrometallurgical process over the conventional roasting process, a brief thermodynamic study was undertaken.

The first step was to determine the thermal conditions in which MnO_2 is reduced to MnO. The Ellingham Diagram[22] provided in Figure 38, is useful in determining the conditions (a combination of temperature and reducing conditions) in which metal oxides can be reduced.

---

[22] Ellingham Diagrams, “An Introduction to Metallurgical Thermodynamics”, David R. Gaskell, McGraw Hill, New York, 1981, p. 287.

Roasting MnO_2 would promote reduction to MnO according to the following reaction:

$$2MnO_2 \rightarrow 2MnO + O_2 \qquad (35)$$

The Gibbs free energy of this reaction can be determined by the following equation:

$$\Delta G_{reaction} = \Delta H_{reaction} - T\Delta S_{reaction} \qquad (36)$$

Using the thermodynamic data summarized in Table 27[12], the Gibbs free energy equation for reduction roasting MnO_2 to form MnO is as follows:

$$\Delta G_{reaction} = 269.8 - 0.219T \quad (KJ/mol);\ T\ (^oK) \qquad (37)$$

By plotting this Gibbs free energy equation on the Ellingham Diagram in Figure 38, the equilibrium line lies near the top of the diagram. As such a reducing atmosphere may not be necessary to reduce MnO_2 to MnO as long as the temperature is high enough.

Burning a fossil fuel with 20% excess air will produce a furnace atmosphere containing a partial pressure of O_2 in the range of 0.032 to 0.035 atm. By intersecting the partial pressure of O_2 equilibrium line (at 0.035 atm O_2) with the Gibbs free energy line for MnO_2 reduction, the intersection point is at about 800 ^oC. As such, by roasting MnO_2 at above 800 ^oC with a furnace atmosphere produced by the complete combustion of a fossil fuel will promote reduction of MnO_2 to MnO. To improve the kinetics of the roasting reaction, a higher temperature would be used (e.g. 900 ^oC).

Using the assumptions listed in Table 28, a breakdown of calculated energy requirements for roasting MnO_2 containing ore is provided in Table 29. Based on the assumptions outlined, over 2 MWh per tonne of Mn could be saved by avoiding roasting and utilizing hydrometallurgical processing instead. In addition to the energy savings achieved by avoiding high temperature reduction roasting, other benefits include the avoidance of pollution control and dust collection from the exhaust streams and avoidance of cooling time required to process roasted ores. Furthermore, it is possible that the milling requirements of crushing and grinding hard high grade MnO_2 ores are much more extensive than for the lower grade, fine grained clayey American Manganese resource material.

Table 27:
Thermodynamic Data[12] for Reduction Roasting Calculations.

Compound	ΔH (KJ/mol)	S (J/mol K)	C_p (J/mol K)
MnO_2	-520.1	53.1	75.1
MnO	-385.2	59.8	54.2
O_2	0	205.152	
SiO_2			68.4

Table 28:
Assumptions for Calculating Energy for Reduction Roasting of Mn Ores

Weight of Mn Production Basis	1 Metric Tonne
Weight % Mn in Ore	35%
Roasting Temperature	900 °C
Mn Mineral	MnO_2
Balance	SiO_2

Table 29:
Breakdown of Calculated Energy Requirements for Roasting Mn Ore

Enthalpy Requirements to Convert MnO_2 to MnO	682 KWh/tonne Mn
Specific Heat Requirements to Heat MnO_2 to 900 °C	445 KWh/tonne Mn
Specific Heat Requirements to Heat SiO_2 to 900 °C	339 KWh/tonne Mn
Losses due to 80% Recovery of Mn	283 KWh/tonne Mn
Losses due to 80% Heat Utilization Efficiency	283 KWh/tonne Mn
Total Energy Usage for Roasting	**2032 KWh/tonne Mn**

Figure 38:
Ellingham Diagram

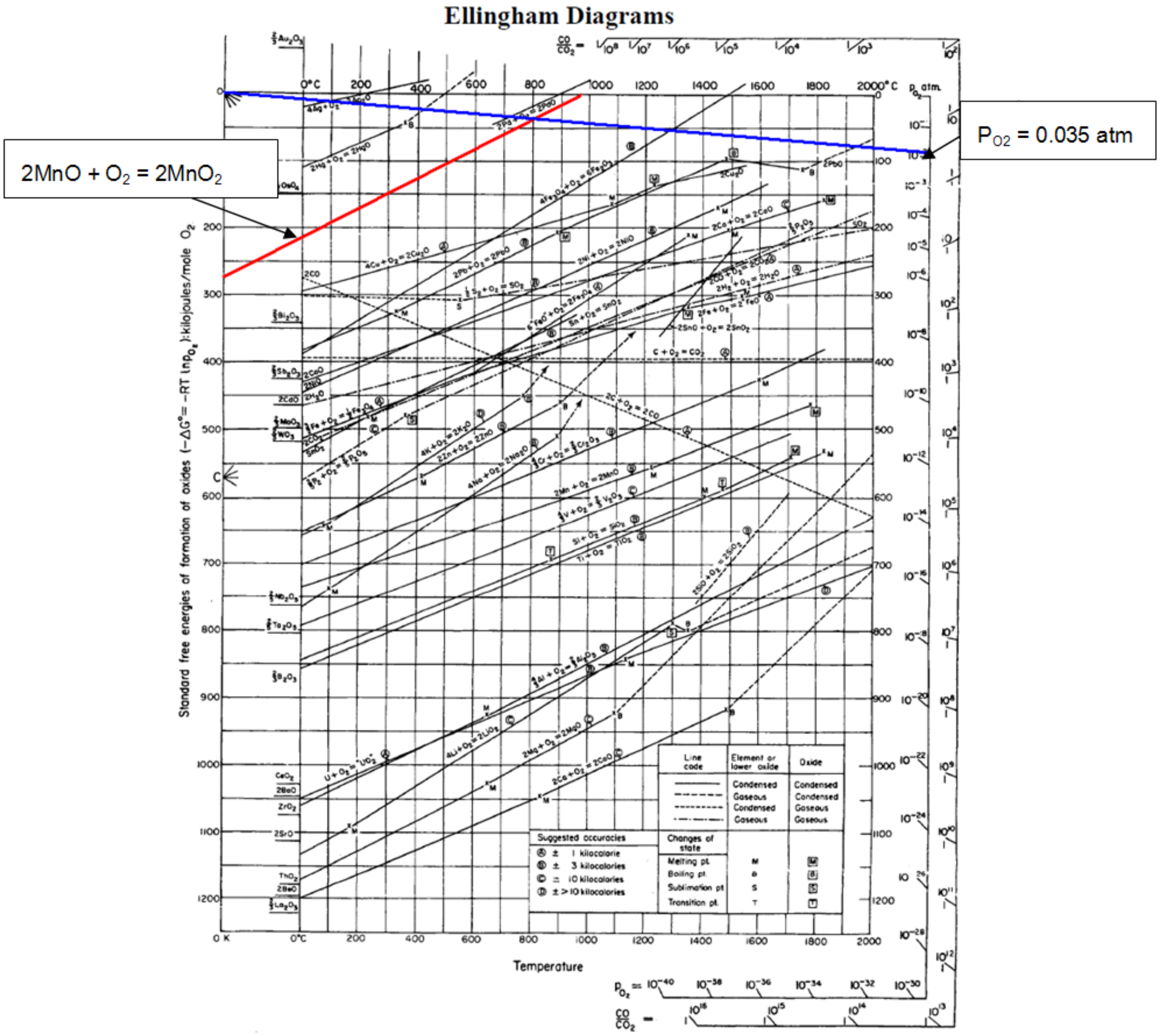

4

CONCLUSIONS

Several conclusions can be drawn from these studies:

Sulphur Burning

1. SO_2 gas is produced on-site by burning elemental sulphur with 20% excess air.
2. Heat exchanging the exhaust gases from the sulphur burner will produce 20 tonnes per hour of steam at 400 ^{o}C and 45 bar pressure.
3. In a condensing turbine, this steam can produce 5 MW of continuous electrical power.

Leaching

4. The Mn mineral in the resource sample provided by American Manganese is primarily pyrolusite and wad (MnO_2), in which the Mn has a 4^+ valence. The insoluble 4^+ valence species of Mn can be readily reduced to soluble 2^+ with SO_2 reducing agent dissolved in water.
5. Leaching studies performed on American Manganese resources of large particle size (greater than 9.5 mm) with dilute SO_2 in stirred tanks indicates that the material is readily leachable, with Mn extractions greater than 90% achieved.
6. The material is friable and large particles break down easily during stirred tank leaching. As such crushing and grinding to a fine particle size prior to leaching is not necessary.

Solid Liquid Separation

7. After leaching the material, the Mn reports as Mn in solution, which can be separated from the Mn depleted leach residue using a thickener.
8. The leached residue collected in the thickener underflow can be rinsed in a counter current decantation (CCD) circuit that is typically used in mineral processing operations.
9. The CCD circuit recovers soluble Mn which is returned to the leach.
10. Settling of the leached solids was best achieved with a lower pulp density (in the range of 12%) along with the use of a non-ionic flocculant.

Pregnant Leachate Solution Purification

11. Solution purification is performed in two stages. In the first stage, the solution pH is adjusted to above 6 to precipitate aluminum (Al), arsenic (As) and most of the iron (Fe) and silica (SiO_2). Air/oxygen sparging during the pH adjustment will improve the Fe removal, by oxidizing the ferrous iron to its ferric form. In the second stage, sulphide precipitation will remove the zinc (Zn), providing a solution of sufficient purity to process into a saleable product.
12. The resource material can be used in the purification stage, by providing sufficient alkalinity to achieve a pH around 6 and precipitate a substantial amount of impurities from solution.

Mn Recovery

13. Mn is separated from the pregnant leach solution (PLS) by precipitation quantitatively as manganese carbonate ($MnCO_3$). This is achieved by mixing sodium carbonate (Na_2CO_3) with the PLS solution.
14. Na_2SO_4 and sodium dithionate ($Na_2S_2O_6$) solution by-product is produced during the precipitation of $MnCO_3$ which filters easily.
15. Dissolving the $MnCO_3$ with recycled electrolyte produces a Mn containing solution that is conducive to producing high grade Mn metal.
16. A scoping electrowinning test using the American Manganese purified leachate yielded a Mn metal product of greater than 99.5% purity.
17. Using typical commercial electrowinning conditions, a sheet of manganese metal was plated over a 24 hour period at a current efficiency of up to 67%. This represents typical commercial performance.
18. The Mn metal was plated without the addition of toxic selenium (Se), which is known to improve current efficiency.

Watery Recovery, Anhydrous Sodium Sulfate Production and Dithionate Destruction

19. Most of the water used in the leaching process is found in the Na_2SO_4 and $Na_2S_2O_6$ solution which is produced during the recovery of $MnCO_3$ by precipitation.
20. Water recovery from this solution can be achieved with high energy efficiency because of the unique solubility characteristics of Na_2SO_4, which enable the majority of Na_2SO_4 to be crystallized as sodium sulphate decahydrate ($Na_2SO_4 \cdot 10H_2O$) simply by cooling the solution. This method is significantly more energy efficient than standard evaporation since it avoids latent heat requirements which accounts for about 85% of the energy required to evaporate water from a starting temperature of 25 ^{o}C.
21. $Na_2S_2O_6$ will report with the $Na_2SO_4 \cdot 10H_2O$ crystals and can be calcined with high energy efficiency since most of the water has been removed. Calcining $Na_2S_2O_6$ will produce anhydrous Na_2SO_4 and recover SO_2 which can be recycled back to the leach.
22. The energy used to recover water, produce anhydrous sodium sulphate and decompose $Na_2S_2O_6$ to recover SO_2 is essentially in balance with the energy provided by the production of sulphur dioxide in the sulphur burning process.

23. Proof of concept was achieved by using a bioreactor technology owned by Kemetco to recover H_2S from $Na_2S_2O_6$. The H_2S can be burned to generate energy and recover SO_2 for leaching. Further development work is required to determine if the reaction rates are adequate for integration into the overall process. Implementation of this technology would further improve the efficiency of the overall process.

Tailings

24. Solid tailings with minimum water content are produced by filtration of the final CCD underflow material, minimizing water requirements for the overall process.
25. The solid tailings produced from test work were shown to be benign by the Toxicity Characteristic Leaching Procedure (TCLP).

Overall Flowsheet

26. A complete flowsheet was developed to extract Mn from lower grade resources by leaching with aqueous SO_2, dealing effectively and efficiently with the dithionate content before producing high grade electrolytic manganese metal and effecting complete control of water and sulphur balances throughout the entire process.

5

REFERENCES

1. Roskill Information Services, "Economics of Manganese", Eleventh Edition, 2008, pp1-2.

2. Kirk-Othmer Encyclopedia of Chemical Technology, 5th Edition, John Wiley & Sons Inc., Volume 15, pp 538 – 565

3. John J. Henn, Ralph C. Kirby, Lindsay D. Norman Jr., "Review of Major Proposed Processes for Recovering Manganese from United States Resources", U.S. Bureau of Mines, Information Circular 8368, 1968

4. John E. Pahlman, Sanaa E. Khalafalla, "Leaching of Domestic Manganese Ores with Dissolved SO2", U.S. Bureau of Mines, RI 9150, 1988

5. A. E. Back, S.F. Ravitz, K.E. Tame, "Formation of Dithionate and Sulfate in the Oxide of SO2 by MnO2 and Air", U.S. Bureau of Mines, RI 4931, 1952

6. Grady Tarbutton, J.C. Driskell, T.M. Jones, F.J Gray, C.M. Smith, "Recovery of Sulfur Dioxide from Flue Gases", Industrial and Engineering Chemistry, Vol. 49, No. 3, 1957, pp 395

7. Karen Voogt, Kathryn C. Sole, and Lesley J. Bryson, "Pilot-Plant Study of Sulfuric Acid Extraction from a Nickel Electrolyte Using Alamine 308", The South African Institute of Mining and Metallurgy, Base Metals Conference, 2009

8. M. Paleologou, R. Thompson, R.M. Berry, C. Brown, M. Sheedy and T. Gilliss, "The Generator Acid Purification (GAP) System Reduces Caustic Make-up Requirements at Kraft Mills", Pulp and Paper Canada, Vol. 100:2, 1999, pp 34 – 39

9. Louis N. Allen, Jr., "Recovery of Manganese from Low-Grade Ores", Chemical Engineering Progress, Vol 50, No. 1, 1954, pp 9 – 13

10. R. Gonzales-Santos, R. Roque-Malherbe, "Dielectric Differential Thermal Analysis; VIII. Dithionates", Journal of Thermal Analysis, Vol. 37, 1991, pp 787-790.

11. Ralph W. M. Lai, Edwin. L. Owen, "Flotation and Sintering of Synthetic Manganese Carbonate", U.S. Patent #4,274,866, Kennecott Copper Corporation, 1981

12. Perry's Chemical Engineers Handbook, 8th Edition, Mcgraw-Hill, 2008, pp 1.237 – 1.298 & 2.156 – 2.163

13. Atlas of Electrochemical Equilibria in Aqueous Solutions, Marcel Pourbaix, Nace Publishing, 1974.

14. Christopher Ward, "Hydrometallurgical Processing of Manganese Containing Materials", PCT Patent Application #WO 2004/033738 A1, HITECH ENERGY LIMITED, 2004.

15. Code of Federal Regulations, http://ecfr.gpoaccess.gov

16. W.F. Linke, A. Seidell, "Solubilities of Inorganic and Metal Organic Compounds", 4th ed., Van Nostrand, 1965.

17. W.C. de Baat, "Sur L'Acid Dithionique et Ses Sels", Recueil des Travaux Chimiques des Pays-Bas, vol 45, 1926, pp 237.

18. Feng Guozhong Lei Yidong, "The Measurements of Thermodynamic Functions of Manganese Dithionate Hydrates", Journal of Guangxi University (Natural Science Edition), Vol. 2, 1992

19. P. Geisler, W. Krumm , and T.A. Peters, "Reduction of the energy demand for seawater RO with the pressure exchange system PES", Desalination, Vol. 135, 2001, pp. 205-210.

20. Von G. Tammann, W. Boehme, "Zur Zersetzung der Dithionate", Zeitschrift Für Anorganische und Allgemeine Chemie, Vol. 204, 1932, pp 144.

21. Donald E. Garrett, "Sodium Sulfate, Handbook of Deposits, Processing, Properties, and Use", Academic Press, 2001, pp 220 – 225.

22. Ellingham Diagrams, "An Introduction to Metallurgical Thermodynamics", David R. Gaskell, McGraw Hill, New York, 1981, p. 287.

6

BIOGRAPHIES

Kemetco Research Inc.

Kemetco Research is privately owned contract Research and Development Company specializing in extractive metallurgy, chemical processing and specialty chemical analysis. Kemetco was formed after the acquisition of the Industrial Process Division of BC Research. BC Research had been in operation for over 60 years as an R&D contractor in British Columbia, Canada.

Kemetco provides laboratory analysis and testing, field work, bench scale studies, pilot plant investigations, consulting services, applied research and development and intellectual property management.

Norman Chow, M.A.Sc., P.Eng.

Norman Chow earned a B.A.Sc. and an M.A.Sc. in Metals and Materials Engineering from the University of British Columbia. He is a Registered Professional Engineer (P. Eng.) in British Columbia. Mr. Chow has over 15 years of technology development and contract research experience. Mr. Chow co-invented a patented electrochemical metal cleaning process that has over fifty installations in twelve different countries with multi-national metal producers. He is the President of Kemetco Research Inc., which he formed after acquiring the Industrial Process Division of BC Research Inc.

Mr. Chow's patented metal cleaning technology was the winner of the Financial Post Gold Award for being the Top Environmental Technology in Canada. In addition, Mr. Chow was the winner of the Business in Vancouver Top Forty under 40 Award, recognizing top business achievers under the age of 40.

Mr. Chow is responsible for developing the water recovery methodology and conducting the mass and energy balances described in this report. Mr. Chow along with Dr. Nacu, authored the majority of this report.

Dr. Anca Nacu, PhD,

Anca Nacu received her B.Sc. and M.Sc. in Chemistry from the University of Timisoara, Romania and subsequently earned a PhD in Chemical Engineering from Taiwan National University. Dr. Nacu is a Project Manager at Kemetco and manages the majority of Kemetco's contract work and testing projects. Dr. Nacu was the project manager for the American Manganese project and was responsible for managing the completion of all test work related to this project. Dr. Nacu along with Mr. Chow authored the majority of this report.

Doug Warkentin, P.Eng.,

Doug Warkentin received a B.A.Sc. in Mining and Mineral Process Engineering from the University of British Columbia and subsequently became a Registered Professional Engineer (P.Eng.) in British Columbia. Mr. Warkentin is a Qualified Person under NI 43-101 for the public reporting of results from metallurgical test programs. Mr. Warkentin manages Kemetco's R&D projects. He has 17 years experience covering a wide range of projects in mineral and biological process engineering, resource recovery, extractive metallurgy and waste treatment. His experience includes plant design, construction, operation, and evaluation as well as process research, development piloting, and project management. Mr. Warkentin has conducted numerous research and testing programs requiring novel flowsheet development, including the development of patentable processes.

Mr. Warkentin was responsible for test program related to the biological reduction of dithionates described in this report.

Igor Aksenov

Igor Aksenov received a Bachelor of Applied Science in Chemical Engineering from Perm State Technical University, Russia. Mr. Aksenov is a process engineer and has been involved in detailed engineering, feasibility studies and plant commissioning of sulphuric acid plants and horizontal belt filters, thickeners and associated mineral processing equipment. Mr. Aksenov's has extensive experience as a process engineer through his work with Aker Solutions, Delkor Global and Shell.

Mr. Aksenov was responsible for test program related to the solid – liquid separation described in this report

Hoe Teh, P.Eng.

Hoe Teh received a B.A.Sc. in Metallurgical Engineering from the University of British Columbia and is currently a Registered Professional Engineer (P.Eng.) in British Columbia. Mr. Teh has 36 years of extensive experience in mineral processing, hydrometallurgy, pyrometallurgy, and environmental operations. His experience covers 8 years in R&D, 17 years in operations, 11 years in engineering & consulting involving scoping to feasibility studies and detailed engineering. Mr. Teh has held senior technical positions with Barrick Gold, Hatch and Teck Resources (formerly Cominco Ltd).

Mr. Teh was responsible for process design and engineering of the conceptual process flowsheet described in this report, in regards to practical operation.